Food and Energy Security

WILEY

Food and Energy Security Open Access

ORIGINAL ARTICLE OPEN ACCESS

Towards Iron Biofortification of Banana (*Musa* spp.): A Comparative Study of Fruit Mineral Micronutrient Concentrations and Phylogenetic Insights Into Iron Homeostasis

Tal Cooper[1] | Amba Phillips[1] | Jeff Daniells[2] | Zachary Stewart[1] | Moses Matovu[3] | Robert Harding[1] | James Langham Dale[1] | Jean-Yves Paul[1]

[1]Centre for Agriculture and the Bioeconomy, Queensland University of Technology, Brisbane, Queensland, Australia | [2]Department of Primary Industries, Agri-Science Queensland, South Johnstone, Queensland, Australia | [3]National Agricultural Research Organisation, National Livestock Resources Research Institute, Kampala, Uganda

Correspondence: Jean-Yves Paul (jy.paul@qut.edu.au)

Received: 31 January 2025 | **Revised:** 1 May 2025 | **Accepted:** 16 May 2025

Funding: This study was supported by the Bill and Melinda Gates Foundation, OPP1178822.

Keywords: banana | biofortification | deficiency | iron | micronutrient | *Musa* | nutrition | staple food crop | Uganda | zinc

ABSTRACT

Iron deficiency anemia (IDA) is alarmingly prevalent in sub-Saharan Africa, where populations often rely on nutrient-poor staple crops as their primary energy source. The East African highland banana (EAHB), a staple for millions in Uganda and most of East Africa's highlands, contains insufficient iron to meet dietary needs. Based on average daily consumption and recommended iron intake, biofortification of EAHBs with upwards of 18.3 mg/kg DW of iron could significantly reduce IDA in these communities. A comprehensive analysis of 43 *Musa* genotypes revealed that, although iron concentrations in banana fruit pulp were generally low, significantly higher concentrations were found in the pulp of wild species and Fe'i cultivars compared with other genome groups. In other tissues, such as the peel and seeds of wild fertile diploids, iron concentrations were consistently higher, underscoring the critical role of this mineral in photosynthesis and seed development. Genomic and phylogenetic analyses across five selected banana cultivars identified 37 genes associated with iron homeostasis, spanning six distinct protein families, and revealed distinct differences between Fe'i and the commercially important cultivar, Cavendish. A tissue-specific differential gene expression study in Cavendish further identified key regulators of iron homeostasis in this crop. These findings provide a foundational resource for the biofortification of this important fruit and contribute to addressing a persistent global health challenge.

1 | Introduction

Iron deficiency is the most prevalent nutrient deficiency in humans and the leading cause of anemia, posing a significant risk to global health (Kumar et al. 2022). With more than half a billion individuals estimated to be suffering from IDA and/or depleted iron stores, the impact of this condition cannot be understated (Johnson et al. 2011). Moreover, iron deficiency disproportionately affects vulnerable populations in resource-limited regions where even mild conditions can result in debilitating health outcomes (Finkelstein et al. 2017; Detzel and Wieser 2015). Uganda, a developing nation situated in the Great Lakes region of East Africa, faces substantial health concerns due to dietary deficiencies in micronutrients, particularly vitamin A, iron, zinc, and iodine. Approximately 53% of Ugandan children under the age of five and 35% of women at reproductive age suffer from IDA (UBOS 2017). Addressing this significant public health challenge will be essential to improve child well-being and development, enhance overall quality of life, and reduce associated mortality rates within these communities.

East African highland bananas (EAHBs) are a genetically distinct group of *Musa* cultivars, primarily triploid (AAA) but also including some diploid (AA) genotypes, cultivated extensively in the Great Lakes region of East Africa (Perrier et al. 2019). They are a dietary staple in Uganda and neighboring countries, with the highest per capita consumption in the world reaching up to 300 kg annually (Fungo 2010). EAHBs are critical to regional food security, providing essential macro- and micronutrients to approximately 30 million people, many of whom are vulnerable to IDA (Perrier et al. 2019; Fungo and Pillay 2011). Unfortunately, the concentrations of essential micronutrients in this major staple are invariably low, ranging from 0.7 to 6.1 mg/kg dry weight (DW) for iron and 0.0 to 5.4 mg/kg DW for zinc (Pillay and Fungo 2016), which has greatly exacerbated the prevalence of IDA and zinc deficiencies in the region (Matovu 2016; Fungo 2010).

Biofortification of staple food crops through conventional breeding or genetic modification has proven to be a sustainable and cost-effective strategy to alleviate iron deficiency. For example, conventionally bred, iron-biofortified pearl millet (Govindaraj et al. 2019), common bean (Katsvairo 2014), and rice (Gregorio et al. 2000) have shown promise in addressing iron deficiency in India, Rwanda, and the Philippines, respectively (Pompano et al. 2022; Haas et al. 2016, 2005). Similarly, cassava (Narayanan et al. 2019, 2015; Taylor et al. 2016), rice (Kawakami et al. 2022; Johnson et al. 2011), and wheat (Beasley et al. 2019; Connorton et al. 2017) have been genetically modified for increased iron content.

In 2005, the Banana21 biofortification project, supported by the Bill & Melinda Gates Foundation, was initiated to help mitigate vitamin A and iron deficiency in Uganda through the micronutrient enhancement of the EAHB using genetic modification (Paul et al. 2017). This approach was considered the most feasible due to the low fertility of edible bananas, which makes conventional breeding difficult (Becker et al. 2000) and the availability of transformation protocols for many banana cultivars (Khanna et al. 2007, 2004). However, unlike other crops such as rice (Wu et al. 2022; Vasconcelos et al. 2017), wheat (Connorton and Balk 2019; Bonneau et al. 2016) and barley (Tauris et al. 2009), the current understanding of mineral homeostasis in bananas is very limited (Yadav et al. 2017).

Iron is not biosynthesized *in planta*, but obtained from the soil; accordingly, plants have evolved intricate mechanisms to regulate its uptake and storage to maintain homeostasis (Briat et al. 1995). Significant progress has been made in improving iron biofortification in various crops through genetic engineering by an in-depth understanding of the molecular processes involved in iron mobilization from the soil, uptake from the rhizosphere, translocation, and redistribution through the aerial tissues, and accumulation in a bioavailable form in edible parts of the plant (Sánchez et al. 2012; Morrissey and Guerinot 2009; White and Broadley 2009). Plants utilize complex strategies to acquire iron from the soil, primarily through two methods: reducing Strategy I and chelating Strategy II (Römheld 1987a). Nongraminaceous monocots such as banana rely primarily on acidification and reduction to access iron from the soil using two key enzymes. These include ferric reductase oxidase (FRO) (Robinson et al. 1999), which reduces ferric ions to ferrous ions, and iron-regulated transporter (IRT) (Vert et al. 2002), which transports iron across root cells. Other important enzymes in the process include nicotianamine synthase (NAS) (Takahashi et al. 2003; Shojima et al. 1990), which catalyzes the production of nicotianamine for iron transport; yellow stripe-like protein (YSL) which aids in the movement of iron complexes within the plant (Koike et al. 2004); vacuolar iron transporter (VIT) which is associated with iron storage in vacuoles (Kim et al. 2006); and ferritin (Fer) which facilitates iron storage in the seeds and leaves, helping manage iron concentrations and prevent toxicity (Theil 2003; Theil et al. 1997).

In many genetically modified (GM) crops, with β-carotene-enhanced Golden Rice being a well-known example, the source of a transgene can greatly influence the desired phenotype (Ye et al. 2000). Similarly, the fruit of Cavendish banana plants over-expressing a *phytoene synthase* gene derived from a Fe'i banana contained higher concentrations of β-carotene equivalents than fruit from transgenic banana plants over-expressing a maize orthologue (Paul et al. 2017). Therefore, investigating the natural variation in fruit mineral concentrations across diverse *Musa* genotypes, including wild and consumed cultivars, may identify valuable genetic resources that could be exploited for iron biofortification. Such studies are currently lacking in many banana genotypes. Wild species are usually considered a valuable genetic resource to enhance the genetic diversity of cultivated crops (Brozynska et al. 2016). As such, investigating *M. acuminata* Colla (AA) and *M. balbisiana* Colla (BB) species, the wild relatives of most edible diploid or triploid hybrid bananas, can inform future decisions made toward banana biofortification. Fe'i bananas are a unique a group of *M. troglodytarum* spp. (T) diploid (TT) and triploid (TTT) cooking cultivars found in the Pacific region, which are easily identifiable by their red or purple sap, deep yellow-orange flesh color, and are particularly renowned for their abundant pro-vitamin A content (Li et al. 2022; Thomson et al. 2022; Buah et al. 2016). These bananas not only have cultural significance to the Pacific region but also potential nutritional value due to their distinct characteristics (Thomson et al. 2022). To date, relatively few studies have been conducted to investigate the mineral content in the fruit of Fe'i (Englberger et al. 2003) and wild banana species, nor has it been measured in the peel and seeds of any *Musa* species.

At the onset of the Banana21 initiative, understanding the genetic basis of iron regulation in *Musa* was identified as a critical step toward developing effective biofortification strategies for this staple food crop. This study aimed to establish whether bananas have the genetic potential to accumulate and regulate nutritionally significant concentrations of iron in their fruit. To guide these efforts, the minimum fruit iron concentration threshold—defined as "the target"—necessary to meaningfully impact populations reliant on bananas as a dietary staple was calculated. To identify potential genetic sources for biofortification, iron and other mineral concentrations in the fruit of 33 *Musa* genotypes were measured, and their natural variation was determined and compared to

10 cultivars commonly grown in Uganda. Furthermore, key genes involved in iron homeostasis were identified in relevant cultivars, and their evolution and expression profiles were analyzed, providing insights into their potential contributions to enhanced iron content.

2 | Materials and Methods

2.1 | Banana Fruit Sample Collection and Handling

A diverse range of 33 *Musa* cultivars was selected that were growing in a germplasm collection maintained by the Queensland Department of Primary Industries (QDPI), South Johnstone Research Station (SJRS, Australia). Mature full green (FG) fruit were harvested from the middle hand of each bunch at least three times over a 4-year period from healthy, individual plants of the same age cultivated under the same field conditions. In instances of high variability between replicates, sampling was increased to up to six replicates. For three Fe'i cultivars, Asupina, Karat, and Taweyawa, samples could only be collected once due to the inconsistent bunching of these genotypes. Fruit were received in the laboratory in Brisbane within 48 h of harvest, photographed, measured, and processed immediately. Bunch weights were compiled from various literature sources and averaged (Smith et al. 2018; Daniells and Hamill 2004; Daniells and Bryde 2001; Arnaud and Horry 1997; Daniells 1986). In addition, FG fruit were also harvested as described previously from 10 cultivars grown in 13 districts in Uganda, representing all agroecological banana growing zones of the country.

2.2 | Banana Fruit Sample Processing for Mineral Analysis and Storage

Fruit were washed with Milli-Q water, dried, separated into peel, pulp, and seed (when available), diced using ceramic knives, placed in 50 mL polypropylene (PP) tubes, and stored at −80°C before being lyophilized. Subsequently, fruit pulp samples were milled to a fine powder using mortar and pestles, sieved using a 0.2 mm plastic mesh, and stored in sealed 50 mL PP tubes with high-density polyethylene (HDPE) screw caps at room temperature (21°C–23°C). Peel and seed samples were milled using a Mixer Mill MM 400 (Retsch) and tungsten carbide grinding jars and stored as previously described. When required, banana samples were artificially ripened at 20°C in sealed opaque polyethylene 50 L containers using ~10 L of 4.5% ethylene in CO_2 (RIPEGAS, BOC) until a fully ripened Stage 6 was achieved as shown in Figure S1 (USDA, AMS, FVP, and SCI 2001).

2.3 | Samples Digestion and Analysis of Mineral Micronutrient Concentration

For the measurement of mineral concentration, 200 mg of dried sample was acid digested essentially as described by Wheal et al. (2011). Every sample was processed in triplicate for mineral analysis. Mineral concentration was measured using inductively coupled plasma optical emission spectrometry (ICP-OES) on a Perkin Elmer ICP-OES 8300DV, configured and protocol implemented as detailed by Pepper et al. (2021). Method robustness, accuracy, and precision were verified by continuing analysis of a certified reference wild-type banana sample (CRM-IPE 929) initially analyzed at Wageningen Evaluating Programs for Analytical Laboratories (WEPAL). Samples were analyzed using an integration time of 0.15 s with three replications. Concentrations were expressed in mg/kg on a dry weight (DW) basis. Samples were checked for high concentrations of heavy and contaminating metals and retested if contamination was suspected.

2.4 | Micro X-Ray Fluorescence Spectroscopy (μ-XRF)

Thin cross-sections of fresh fruit from Zebrina were prepared using a ceramic knife. μ-XRF elemental mapping was performed at the Centre for Microscopy and Microanalysis (University of Queensland) with the ATLAS X micro XRF Spectrometer (IXRF Systems, USA). Measurements were conducted at room temperature (~20°C) using the 25 μm Molybdenum anode x-ray source at a 40–50 kV, 1000 μA, with a rise time of 0.25 μs and a per-pixel dwell of 50–100 ms. A Silicon Drift Detector (SDD) was used to capture the full fluorescence signal. Elemental maps were generated using the IXRF Iridium Ultra and GeoPIXE software packages, using the sum of counts at the position of the principal peak for each element. These were each exported into ImageJ as grayscale 8-bit TIFF files, internally normalized such that each image covered the full dynamic range, and final images were colored using Imaris 9.3 (Oxford instruments).

2.5 | Statistical Analysis

All statistical comparisons were made using R (ver. 3.5.0, R Foundation for Statistical Computing, Vienna, Austria). Normality and homogeneity of variances were tested with D'agostino-Pearson and Levene's tests, respectively. For retention studies, the Mann–Whitney *U* test was used to test the variance of the two groups. In all other instances, analysis of variance was done using the non-parametric Kruskal–Wallis H test, with multiple comparisons made with Dunn's post hoc test and *p* values adjusted with the Benjamini–Hochberg method. Statistical significance was asserted at 95% confidence ($p > 0.05$) for all tests. These tests were performed with base R and packages fBasics ver. 3042.89.2, DescTools ver. 0.99.45, FSA ver. 0.9.3, and car ver. 3.1-0. Pearson's correlation and correlogram graphs were generated using corrplot ver 0.92. Estimation statistics and Gardner–Altman plots were generated using dabestr ver. 0.2.5. Principal component analysis (PCA) and subsequent biplots and modelling generated were performed using factoextra ver. 1.0.6.

2.6 | Identification and Naming of Iron Homeostasis Genes From DH Pahang

To identify genes associated with iron homeostasis (*Fer*, *FRO*, *IRT*, *NAS*, *VIT*, and *YSL*), the amino acid sequences of these well-characterized genes in *Arabidopsis thaliana* and *Oryza sativa* (Table S1) were used as queries for BLAST searches against the DH Pahang ver. 4 annotated banana genome available on the Banana Genome Hub (Belser et al. 2021). When matching banana sequences were significantly longer than their counterparts in *A. thaliana* and *O. sativa*, putative genes from the same chromosomal region in the DH Pahang ver. 2 assembly but with the correct sequence size were substituted (Martin et al. 2016). Each identified putative *Musa* iron homeostasis gene was assigned a unique name using the assembly description as default. Homologous sequences with a generic assembly description were discriminated with an extension consisting of (1) a number starting with the lowest possible number and in order of chromosomal location and (2) a letter (a, b, c…) for each paralogue in order of location on the same chromosome.

2.7 | Iron Homeostasis Gene Prediction in Other Cultivars

Using Liftoff ver. 1.6.3 (Shumate and Salzberg 2021), putative iron homeostasis gene sequences identified in the DH Pahang ver. 4 and ver. 2 assemblies (Table S1) were used to predict homologous and orthologous sequences from four *Musa* and two *Ensete* (outgroups) cultivar assemblies. Initially, putative sequences identified in the ver. 2 annotation replaced their incorrectly sized ver. 4 assembly counterparts using Liftoff. Subsequently, all sequences were extracted from this hybrid annotation. Genome assemblies of the selected cultivars were downloaded from the Banana Genome Hub (Droc et al. 2013), and orthologous gene sequences were annotated using the newly created hybrid annotation. All cultivar/accession/species selected for analysis and the subsequent abbreviations used to refer to them can be found in Table S2.

2.8 | Sequence Alignment and Phylogenetic Analyses

For each iron-regulating gene family (*Fer*, *FRO*, *IRT*, *NAS*, *VIT*, and *YSL*), all homologous and orthologous sequences identified were translated, inspected for redundancy, and manually adjusted. This corrected Liftoff errors, such as extraneous sequences upstream of the true methionine start site to ensure alignment with the open reading frame (ORF) of the hybrid annotation sequences. For phylogenetic analysis, sequences were aligned using ClustalW ver. 2.1 (Thompson et al. 1994) to either generate protein family-level trees or individual protein-level trees. For protein family-level trees, all homologous sequences within each protein family were first concatenated for each banana cultivar prior to alignment. Sequences from Fer2, Fer3b, FRO2b, VIT1b, YSL6a, YSL8, YSL12e, and YSL12g were excluded from concatenation due to premature or multiple stop codons (hereafter referred to as "non-functional"). In addition, as VIT1a and VIT4 were absent in the Utafan assembly, corresponding orthologous sequences from all other cultivars were removed before concatenation. Given the limited number of IRT sequences identified, all were retained, including nonfunctional ones. Proteins from both the *Ensete ventricosum* "Eg" and *E. glaucum* "Ev" assemblies were concatenated to use as the "outgroup." Phylogenetic analyses of individual and concatenated protein sequences were performed using maximum likelihood and the Akaike Information Criterion as implemented in ModelFinder within IQ-TREE ver. 2.2.6 (Minh et al. 2020; Kalyaanamoorthy et al. 2017). Final consensus trees were visualized with FigTree ver. 1.4.4.

2.9 | RNA-Seq Analysis

In house RNA-seq data from two biological fruit replicates of Cavendish (one each from cultivars Grande Naine and Williams) and three biological replicates of leaf and root samples of the Grande Naine cultivar were used for differential gene expression analysis. RNA-seq library quality was assessed using the Fastqc ver. 0.11.2 (Andrews 2010) before alignment. Using a high-performance computer (HPC) the sequences were aligned to the previously described hybrid annotation using kallisto ver. 0.46.1 (Bray et al. 2016) and estimated read counts calculated. Read counts were normalized between samples with DeSeq2 ver. 1.41.0, replicate data averaged, and outliers removed. Relative expression pattern was represented on heats maps that were constructed with the R package pheatmap ver. 1.0.12.

3 | Results and Discussion

3.1 | A Biofortification Target for a Significant Nutritional Impact

The banana fruit iron concentration target was calculated to provide at least 50% of the estimated average requirement (EAR) (Bouis et al. 2011; White and Broadley 2009). Daily requirements for absorbed iron vary depending on the age and sex of the target population (Table 1); nevertheless, absorption is influenced by three independent factors: food intake (g/day), retention (losses through processing), and bioavailability (Bouis et al. 2011; White and Broadley 2009).

The consumption of cooking banana in Uganda is the highest in the world, with reports in excess of 1 kg per person per day (Fungo 2010). In the absence of reliable and detailed banana consumption references for different age groups in Uganda, the consumption of cooked banana (the national dish, matoke) was conservatively estimated and adapted for each age group (Table 1) (García et al. 2015; NHMRC et al. 2006). In Uganda, matoke is prepared by either boiling or steaming peeled banana fruit for at least an hour before mashing. When the iron and zinc content of Cavendish banana fruit pulp boiled for 1 h in water was compared to that of the unboiled equivalent, no significant ($p > 0.05$) losses could be attributed to this processing technique (Table S3). Finally, previous work in collaboration with our laboratory has shown an absorption rate of 34% from cooked Cavendish banana (García et al. 2015). From this information, it was estimated that between 8.8 to 18.3 mg/kg DW of iron was required in biofortified banana to achieve 50% of the iron EAR in various age groups (Table 1). Considering that the iron content in the fruit of EAHB cultivars is consistently reported to average around 10 mg/kg DW (Matovu 2016), age groups such as adult males and women past their 50s probably already benefit greatly from these bananas due to either the large amount of daily banana consumption or the reduced requirement for absorbed iron, respectively. On the other hand, children and women of childbearing age,

TABLE 1 | Potential dietary contribution of cooking bananas to the EAR for iron.

Age group (years)	EAR for iron (mg/day)[a]	Requirement for absorbed iron (μg/day)[b]	Absorbed iron required to meet 50% of the EAR (μg/day)	Banana consumption (fingers/day)	Banana consumption (g FW/day)[c]	Banana consumption (g DW/day)[d]	BC^{50} (mg/kg DW)
Infants							
7–12 months	7	1260	630	1	120	30	61.8
Children							
1–3	4	560	280	1.5	180	45	18.3
4–8	4	720	360	2.0	240	60	17.6
9–13	6	1080	540	3.0	360	90	17.6
14–18	8	1440	720	4.0	480	120	17.6
Men							
19+	6	1080	540	6.0	720	180	8.8
Women							
19–50	8	1440	720	5.0	600	150	14.1
51+	5	900	450	5.0	600	150	8.8
Pregnancy							
14–18	23	4140	2070	4.0	480	120	50.7
19–50	22	3960	1980	5.0	600	150	38.8
Lactation							
14–18	7	1260	630	4.0	480	120	15.4
19–50	6.5	1170	585	5.0	600	150	11.5

Abbreviations: DW, dry weight; EAR, estimated average requirement; FW, fresh weight.

Note: BC^{50}, banana fruit iron concentration needed to achieve 50% of the iron EAR, expressed in mg/kg DW and calculated as follows: $BC^{50} = \frac{I}{(C \times R \times A)}$, I = absorbed iron required to meet 50% of the EAR (μg/day); C = banana consumption (g DW/day); R = cooking retention of 100% (Table S3); A = absorption of 34% (García et al. 2015).

[a] EARs are set by modeling the components of iron requirements, estimating the requirements for absorbed iron at the 50th centile with use of an upper limit of 14% iron absorption for the children 1–3 years of age group and 18% for other age groups, with rounding (NHMRC et al. 2006).

[b] Based on 14% and 18% bioavailability in the diet of children 1–3 years of age and other age groups, respectively.

[c] Based on an average banana finger weight of 120 g FW.

[d] Assuming 25% dry matter.

with a higher requirement for iron (kg for kg) and/or a much smaller consumption habit, are clearly not benefiting from the current cultivars. Our calculation aimed at supporting these two groups who are particularly at risk of micronutrient deficiencies because of their higher nutritional needs for growth and reproductive health (Bouis et al. 2011). The young children (1–3 years) population is by far the most vulnerable group to any sort of nutrient deficiency and to IDA in particular. According to the assumptions and calculations made, consuming bananas with iron concentrations of at least 18.3 mg/kg DW could provide around 50% of EAR for iron to this age group (Table 1), which should result in significant improvement in overall health and development. Similarly, the next most vulnerable group, women of reproductive age, could also obtain 50% of the iron EAR by consuming bananas with iron concentrations of at least 14.1 mg/kg DW. Overall, the data suggest that for most age groups to benefit from an iron biofortified EAHB, the minimum concentrations required would be in the range of 14.1 to 18.3 mg/kg DW, with the higher threshold representing a more pragmatic and beneficial goal, aiming to assist the most nutritionally vulnerable members of the community.

3.2 | Iron and Zinc Concentration in the Fruit Tissues of *Musa* Cultivars

Most studies on fruit mineral concentration in bananas have focused on commonly consumed cultivars, with reported iron concentrations rarely exceeding 10 mg/kg. To date, no banana cultivar has been reported with fruit iron concentrations approaching the calculated target required for biofortification. To assess the fruit iron concentrations in more diverse and lesser-known banana cultivars, iron and zinc concentrations were measured in fruit from 33 *Musa* cultivars grown in a single germplasm collection in Australia. These cultivars ranged from widely consumed dessert bananas like Cavendish (AAA) to more exotic cultivars, including cooking bananas, plantains, Fe'i bananas, and wild fertile diploids, encompassing a wide range of ploidy and genome groups (Table 2). The diversity of fruit phenotypes is shown in Figure 1, with wild fertile diploids producing significantly smaller fruits filled with hard seeds, in contrast to other cultivars. To complete this study, a large set of fruit pulp samples was also collected from farm-grown bananas in Uganda. These included four true EAHB cultivars and one EAHB hybrid as well as one plantain and four dessert varieties included for comparison purposes with the Australian-grown plants (Table 2).

Initially, the iron and zinc concentrations in full green (FG) fruit were analyzed for a subset of 23 cultivars representing all six genome groups. These concentrations were compared to those from artificially ripened equivalent fruit. Regardless of ripeness, no differences were observed in the pulp, peel, or seeds (when available) of any cultivar (Figures S2 and S3). This suggests that the mineral content of banana peel, pulp, and seeds remains stable postharvest and aligns with findings by Aquino et al. (2014), who reported no significant differences in iron content between unripe and ripe bananas across 15 cultivars. Consequently, further analyses were conducted solely on FG fruit.

To understand the relationship between mineral transport from source to sink in banana fruit, the concentrations of iron and zinc were analyzed and compared in three types of fruit tissues, namely pulp, peel, and seed (when available). Data averaged across all cultivars revealed a general trend: Both minerals were found in higher concentrations in the seed, followed by the peel, and lowest in the pulp (Figure 2A,B). Specifically, the pulp contained an average iron concentration of 10.2 mg/kg DW, in contrast to 29.4 mg/kg in the peel and 38.0 mg/kg in the seed (Figure 2A). A similar trend was observed for zinc, with notably higher concentrations in the peel and seed (Figure 2B). Due to their respective roles as a photosynthetically active tissue or as nutrient storage organs, the peel and seed were expected to contain elevated concentrations of iron and zinc, which was confirmed by our analysis. Out of the 33 cultivars analyzed, only the wild *Musa balbisiana* var. Lal Velchi contained more zinc in its pulp than in its peel. Importantly, seeds from these cultivars contained the highest concentration of iron and zinc reported in any banana fruit tissue, demonstrating their importance for iron sequestration within the fruit. Averaging data from unrelated cultivars across multiple genome groups, however, resulted in significant variation in mineral content, clearly demonstrating a lack of uniformity in mineral composition within the genus *Musa*.

When the fruit pulp data were analyzed, the four wild cultivars contained a higher iron and zinc concentration than the other genome groups with an average of 16.9 and 20.8 mg/kg DW, respectively (Figure 2C,D). These differences in fruit iron concentration were significant when compared to all the edible cultivars except those of the Fe'i group. The average concentration of zinc in the fruit of the wild fertile diploids was significantly different to that of all genome groups except that of the AA edible diploids and Fe'i cultivars. The highest concentration of zinc was measured in the pulp of Borneo (31.6 mg/kg DW) followed closely by Zebrina (27.0 mg/kg DW) and Lal Velchi (23.0 mg/kg DW) (Table 2). *Malaccensis* 845 had the lowest zinc concentration of all the wild fertile cultivars containing only 9.1 mg/kg DW, a value that was close to most seedless cultivars.

Only fruit from Zebrina contained iron concentrations above the "target" at 28.9 mg/kg DW, followed by Borneo (16.1 mg/kg DW), Lal Velchi (15.5 mg/kg DW), and 845 (12.5 mg/kg DW) (Table 2). For Zebrina, pulp iron concentrations ranged between 20.2 to 35.3 mg/kg DW. This variation may in part be explained by the lack of homogeneity in the pulp samples collected from wild cultivars. The presence of seeds in these cultivars causes a reduction in the size of the mesocarp and a more pronounced endocarp than what is commonly observed from parthenocarpic cultivars (Figure 3A). As such, the heterogeneity of this matrix and possible seed coat contamination during sampling may have led to the higher variability in pulp iron content seen in the wild cultivars. However, given the important role of iron during the initial heterotrophic phase of development of germinating seedlings, the high concentrations of pulp iron and zinc observed in wild fertile diploids compared to the parthenocarpic diploid and triploid cultivars were not unexpected. Zebrina had both the highest seed iron (61.3 mg/kg DW) and zinc (65.8 mg/kg DW) content (Table 2) while Lal Velchi and 845 had the lowest iron and zinc, respectively. For this reason, fruit from Zebrina was selected for x-ray fluorescence spectroscopy (μ-XRF) and elemental maps used to visualize the localization of iron, zinc, and manganese in the fruit of Zebrina (Figure 3). Iron was found to localize near and around the embryo tip of the fully mature ovules (seed) (Figure 3B,E). Specifically, the highest iron signals were detected in the hilum, micropyle, and micropylar plug of the seed coat and the surrounding area, while very little signal was seen in the endosperm (McGahan 1961). Zinc was uniformly distributed throughout the entire ovary, particularly the vascular tissues, epicarp, mesocarp, and endocarp of the fruit, as well as the endosperm and chalazal mass of the seed (Figure 3C). Manganese, included here as the concentration in Zebrina fruit tissues exceeded 1000 mg/kg cumulatively, localized primarily to the epicarp and carpel walls, allowing clear observation of the individual locule and the overall pistil of the banana ovary (Figure 3D). A composite image of all three elements reveals the tight regulation of iron, mainly concentrated in and around the seed, and also of manganese localized to the septal tissue, while zinc is not nearly as tightly controlled, being distributed diffusely within the fruit tissues of the banana plant (Figure 3E). These findings, demonstrating the localized distribution of iron and the diffuse distribution of zinc, are consistent with the patterns observed in rice grain (Johnson et al. 2011), and highlight the meticulous control of iron homeostasis in bananas, likely as a protective measure against the harmful effects of reactive oxygen species (ROS) on plant health (Arosio et al. 2009). Nevertheless, parthenocarpic bananas such as Cavendish lack the sink capacity of the seed, which may explain the lower concentrations of iron found in these cultivars.

The group of Pacific Fe'i bananas was the next highest accumulator of fruit iron and zinc, with average concentrations of 12.2 and 13.2 mg/kg DW, respectively (Figure 2B,C). The pulp iron concentration was significantly different ($p < 0.01$) to all other edible genome groups (Figure 2A). Due to the higher variation of pulp zinc concentration in these cultivars, significant differences were only observed with the AAA ($p < 0.01$), AAB ($p < 0.001$) and ABB ($p < 0.05$) cultivars (Figure 2B). Although only a single biological replicate was available for the Taweyawa and Karat cultivars, the former had the third-highest fruit pulp

TABLE 2 | Iron and zinc concentration in the fruit of sampled *Musa* cultivars.

Genome group	Subgroup	Cultivar/ variety	*n*	Origin	Pulp		Peel		Seed		Finger width (cm)	Finger length (cm)	Bunch weight[b] (kg)
					Fe (mg/ kg)	Zn (mg/ kg)	Fe (mg/ kg)	Zn (mg/ kg)	Fe (mg/ kg)	Zn (mg/ kg)			
AA (Edible diploid)	N/A	Paka	3	Australia	8.4 ± 0.4	8.0 ± 1.0	22.1 ± 2.2	23.4 ± 1.1	—	—	3.2 ± 0.1	21.1 ± 0.3	16.3 ± 3.3[d]
	Sucrier	Terema	3	Australia	8.2 ± 1.4	8.2 ± 1.3	35.4 ± 7.7	51.5 ± 6.4	—	—	2.9 ± 0.2	9.9 ± 0.4	9.3 ± 5.2[c,g]
AAA	Cavendish	Grande Naine	3	Australia	9.1 ± 1.5	7.2 ± 0.6	34.9 ± 9.8	34.2 ± 2.7	—	—	3.6 ± 0.1	18.6 ± 2.8	37.5 ± 7.1[e]
	Cavendish	Williams	6	Australia	9.1 ± 1.0	6.4 ± 1.3	24.4 ± 7.3	30.5 ± 7.6	—	—	3.6 ± 0.1	18.4 ± 2.9	37.5 ± 7.1[f,g]
	Cavendish	Dwarf Cavendish	1	Australia	11.9 ± 0.7	6.2 ± 0.5	35.6 ± 0.3	70.7 ± 1.7	—	—	3.6 ± 0.0	17.4 ± 0.0	37.5 ± 17.7[c]
	Cavendish	D5	2	Australia	11.8 ± 0.0	8.0 ± 1.3	27.2 ± 1.8	33.4 ± 1.1	—	—	3.6 ± 0.1	20.8 ± 0.6	26.3 ± 5.3[e]
	Cavendish	DPM25	1	Australia	8.6 ± 0.4	6.3 ± 0.1	30.0 ± 0.7	39.2 ± 1.7	—	—	3.5 ± 0.0	21.8 ± 0.0	—
	Cavendish	Valery	1	Australia	9.4 ± 0.2	9.4 ± 0.7	39.9 ± 0.3	54.1 ± 0.7	—	—	3.1 ± 0.0	24.9 ± 0.0	25.4 ± 3.7[e]
	Cavendish	Dwarf Cavendish	27	Uganda	10.9 ± 1.2	6.7 ± 0.9	—	—	—	—	—	—	—
	Gros Michel	Bogoya	30	Uganda	11.1 ± 1.2	5.7 ± 0.5	—	—	—	—	—	—	—
	Rio	Kluai Hom Thong Mokho	4	Australia	8.8 ± 1.2	6.6 ± 1.2	23.2 ± 7.1	36.1 ± 3.9	—	—	3.3 ± 0.3	17.1 ± 1.6	18.4 ± 8.0[d,f]
	Lakatan	Lakatan	4	Australia	9.3 ± 1.8	7.6 ± 1.4	25.9 ± 8.1	22.6 ± 2.5	—	—	3.4 ± 0.1	17.7 ± 2.5	23.1 ± 2.1[d]
	N/A	Pisang Susu	4	Australia	9.2 ± 0.6	6.2 ± 0.3	19.6 ± 3.1	32.7 ± 1.8	—	—	3.8 ± 0.2	13.2 ± 1.3	14.7 ± 6.0[d]
	Red	Red Dacca	3	Australia	7.9 ± 0.9	6.4 ± 1.7	20.9 ± 3.7	35.2 ± 6.2	—	—	4.3 ± 0.3	15.5 ± 0.9	23.5 ± 5.6[c]
	Ibota	Yangambi km5	3	Australia	8.6 ± 1.7	6.2 ± 0.9	24.9 ± 4.7	49.0 ± 7.7	—	—	3.0 ± 0.3	12.8 ± 3.3	23.8 ± 10.5[d]
AAA-EAHB	Mutika/Lujugira	Kisansa	24	Uganda	11.4 ± 1.0	8.2 ± 1.5	—	—	—	—	—	—	—
	Mutika/ Lujugira hybrid	M9	24	Uganda	11.6 ± 1.4	7.5 ± 2.9	—	—	—	—	—	—	—
	Mutika/Lujugira	Mbwazirume	39	Uganda	10.7 ± 2.8	7.9 ± 1.6	—	—	—	—	—	—	—
	Mutika/Lujugira	Nakitembe	33	Uganda	10.1 ± 2.3	8.0 ± 1.5	—	—	—	—	—	—	—
	Mutika/Lujugira	Mpologoma	33	Uganda	10.5 ± 2.2	7.1 ± 0.7	—	—	—	—	—	—	—
AAB	Pome	Lady Finger	4	Australia	8.1 ± 0.5	4.8 ± 1.2	44.6 ± 15.7	43.0 ± 2.1	—	—	3.4 ± 0.3	13.0 ± 0.4	20.0 ± 14.1[c]
	Sukali Ndiizi	Kamaramasenge	27	Uganda	9.4 ± 1.6	5.5 ± 1.0	—	—	—	—	—	—	—
	Plantain	Dwarf French Plantain	4	Australia	8.8 ± 0.5	5.2 ± 0.7	27.8 ± 4.3	38.1 ± 14.9	—	—	3.8 ± 0.1	21.3 ± 0.5	21.2 ± 2.9[d]
	Plantain	Gonja Nakatansese	28	Uganda	12.1 ± 2.6	6.0 ± 1.7	—	—	—	—	—	—	—
	Laknau	Mangat	3	Australia	8.1 ± 2.2	4.9 ± 1.3	22.1 ± 4.4	39.6 ± 3.0	—	—	4.0 ± 0.2	23.2 ± 0.6	13.8 ± 4.4[e,g]
	Maoli/Popoulu	Pacific Plantain	3	Australia	6.9 ± 0.4	7.1 ± 0.6	20.1 ± 1.9	29.1 ± 8.5	—	—	4.7 ± 0.4	19.9 ± 1.3	18.5 ± 2.1[e]
	Pisang Raja	Pisang Raja	3	Australia	7.6 ± 1.7	5.9 ± 0.8	28.2 ± 5.8	40.1 ± 10.2	—	—	3.5 ± 0.2	15.6 ± 1.0	19.8 ± 5.0[c]
	Silk	Sugar	3	Australia	6.3 ± 1.1	4.6 ± 0.5	22.5 ± 10.9	31.9 ± 6.6	—	—	3.3 ± 0.2	12.0 ± 1.6	16.0 ± 7.9[c]
	Iholena	Tigua	4	Australia	7.6 ± 0.3	9.5 ± 1.3	30.1 ± 20.4	44.5 ± 11.7	—	—	4.1 ± 0.5	17.2 ± 2.6	17.9 ± 5.7[g]
ABB	N/A	Da Jiao	4	Australia	8.0 ± 1.3	8.0 ± 1.1	45.3 ± 23.4	31.3 ± 9.9	—	—	3.9 ± 0.2	16.5 ± 1.7	17.4 ± 2.0[d]
	Pisang Awak	Ducasse	4	Australia	8.4 ± 0.9	5.1 ± 0.7	45.3 ± 7.1	52.1 ± 4.7	—	—	3.7 ± 0.1	14.8 ± 1.1	28.3 ± 5.8[c]
	Monthan	Monthan	3	Australia	8.4 ± 1.0	6.8 ± 0.9	26.7 ± 13.2	24.0 ± 8.9	—	—	4.3 ± 0.5	17.0 ± 2.6	15.1 ± 17.8[d]
	Saba	Pisang Gajih Merah	3	Australia	8.8 ± 2.0	8.4 ± 1.9	35.4 ± 3.2	28.0 ± 12.3	—	—	3.9 ± 0.4	15.4 ± 0.3	22.9 ± 2.6[d]
	Bluggoe	Kivuvu	21	Uganda	11.2 ± 1.7	6.9 ± 0.8	—	—	—	—	—	—	—
Fe'i (T)	N/A	Asupina (TTT)	1	Australia	13.3 ± 0.4	10.7 ± 0.5	21.1 ± 0.5	19.6 ± 0.1	—	—	4.4 ± 0.0	16.8 ± 0.0	10.2 ± 5.1[g,h]
	N/A	Karat (TTT)	1	Australia	14.4 ± 0.3	24.8 ± 1.6	18.0 ± 0.4	37.8 ± 1.2	—	—	4.0 ± 0.0	12.2 ± 0.0	12.5 ± 3.5[e]
	N/A	Taweyawa (TT)	1	Australia	15.7 ± 0.2	24.3 ± 0.5	19.8 ± 0.4	32.4 ± 0.1	—	—	4.9 ± 0.0	23.5 ± 0.0	3.0 ± 1.4[e]
	N/A	Utafan (TT)	3	Australia	11.6 ± 1.5	12.8 ± 3.0	24.9 ± 9.7	27.3 ± 10.2	—	—	6.0 ± 0.8	27.2 ± 2.8	22.2 ± 2.6[g,h]
	N/A	Yesing (AT)[a]	3	Australia	10.6 ± 0.5	7.0 ± 1.2	35.6 ± 4.0	65.5 ± 3.8	—	—	3.0 ± 0.6	15.4 ± 4.6	15.7 ± 4.0[e]
Wild (Fertile diploid)	*M. a.* ssp. *malaccensis* (AA)	845	6	Australia	12.5 ± 0.8	9.1 ± 1.0	34.3 ± 5.4	21.8 ± 6.0	37.4 ± 4.8	40.6 ± 11.8	2.0 ± 0.2	8.5 ± 1.0	3.0 ± 0.9[h]
	M. a. ssp. *microcarpa* (AA)	Borneo	4	Australia	16.1 ± 2.6	31.6 ± 16.5	36.4 ± 5.0	59.7 ± 9.2	38.0 ± 12.9	60.2 ± 12.8	1.7 ± 0.1	9.5 ± 1.1	2.5 ± 1.4[d]
	M. a. ssp. *zebrina* (AA)	Zebrina	3	Australia	28.9 ± 7.8	27.0 ± 8.3	31.5 ± 8.3	60.2 ± 21.9	61.3 ± 16.1	65.8 ± 14.0	2.1 ± 0.1	8.2 ± 0.9	2.4 ± 1.2[h]
	M. b. (BB)	Lal Velchi	4	Australia	15.5 ± 6.0	23.0 ± 14.4	18.0 ± 6.3	20.3 ± 5.0	21.4 ± 7.1	53.7 ± 33.5	3.2 ± 0.2	12.9 ± 0.4	8.9 ± 3.9[h]

Note: Data expressed as mean of *n* ± standard deviation (SD). When *n* = 1, SD calculated from the technical replicates. Fe and Zn data calculated on a dry weight basis. Abbreviations: Fe, iron; *M. a.*, *Musa acuminata*; *M. b.*, *Musa balbisiana*; *n*, numbers of biological replicates; N/A, not applicable; Zn, zinc.

[a] *M. acuminata* (A) × *M. troglodytarum* (T) hybrid.

[b] Bunch weight compiled from literature and averaged.

[c] Daniells (1986).

[d] Daniells and Bryde (2001).

[e] Daniells, J.W. personal communication.

[f] Smith et al. (2018).

[g] Arnaud and Horry (1997).

[h] Daniells and Hamill (2004).

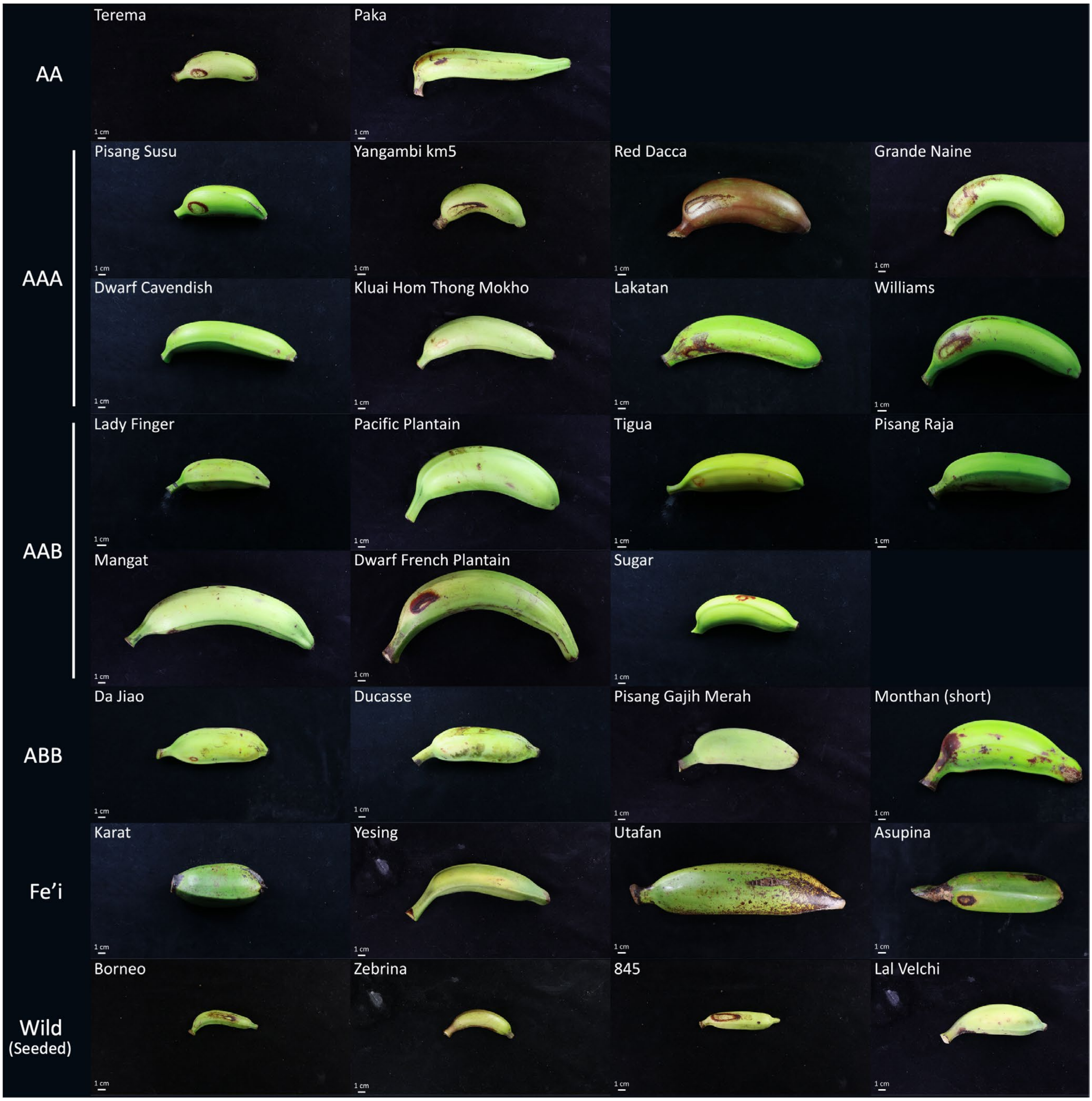

FIGURE 1 | Photographs of *Musa* fruit collected and analyzed. Samples courtesy of Mr. Jeff Daniells (QDPI). Scale bar = 1 cm. Photographs of the fruit of cultivars DPM25, D5, Valery and Taweyawa could not be taken.

iron concentration (15.7 mg/kg DW) and the fourth-highest zinc concentration (24.3 mg/kg DW). Karat's fruit contained similar concentrations, with iron (14.4 mg/kg DW) ranking fifth and zinc (24.8 mg/kg DW) ranking third when compared to all the cultivars analyzed (Table 2). The only promising edible banana cultivars that met the 50% iron EAR for nonpregnant women were Karat and Taweyawa. The fruit from these cultivars also had zinc concentrations far exceeding any values previously reported in edible bananas (Davey et al. 2009). Both of these cultivars as well as Asupina were the only parthenocarpic bananas to have pulp with higher concentrations of iron and zinc than most EAHBs. However, it must be noted that the fruit from these cultivars was only analyzed once. Regardless, Fe'i cultivars consistently outperformed their diploid and triploid (AA, AAA, AAB, ABB) counterparts in terms of nutritional content, yielding fruit with elevated concentrations of both iron and zinc. While very speculative, this superior nutritional profile might stem from their distinct "T" genotype (*Musa troglodytarum* L). Though data on the fruit mineral content of Fe'i cultivars is limited, it is clear they possess significantly higher amounts of carotenoids than the AAA cultivars, such as Cavendish (Buah et al. 2016). This heightened accumulation of nutrients is believed to be partially attributable to an increased storage sink strength within these cultivars, facilitated by a greater number

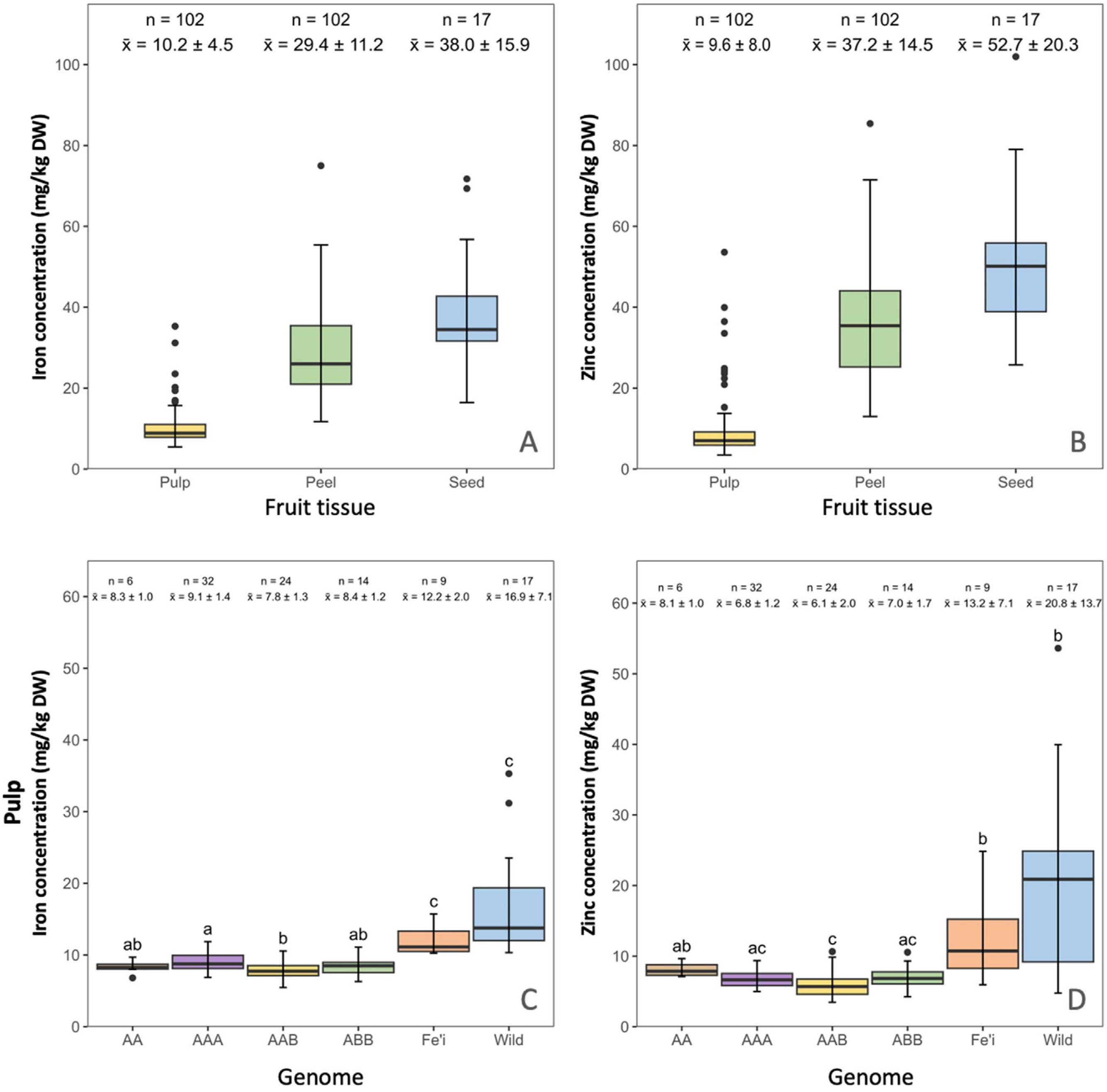

FIGURE 2 | Iron and zinc concentration in the fruit of *Musa* cultivars. (A) Iron and (B) zinc concentrations averaged for each fruit tissue type collected across all cultivars. (C) Iron and (D) zinc fruit pulp concentrations averaged for each genome group. Statistical difference comparing genome groups: Two-way Kruskal–Wallis H test using the Dunn's post hoc test with p values adjusted using the Benjamini–Hochberg method, different letters indicate significant difference ($p < 0.05$). Box and whisker plot interpretation: Each box spans the interquartile range with the ends of the box being the upper and lower quartiles. The median is represented by a horizontal line inside the box. The whiskers are the two lines outside the box that extend to the highest and lowest observations. DW, dry weight; n, number of biological replicates. Data expressed as mean ($\bar{x}$) of $n \pm$ standard deviation.

of plastids in the fruit's pulp (Buah et al. 2016). Consequently, this might also explain the enhanced concentration of both iron and zinc in the pulp of these fruit, whereas the mineral content of the peel remains comparable to that of other cultivars analyzed across various genotypes.

Fruit pulp iron and zinc concentrations in the AAA banana genome group from Australia, which contains the popular Cavendish cultivars, averaged at 9.1 and 6.8 mg/kg DW (Figure 2C,D). This set also contains samples of Dwarf Cavendish and Bogoya (commonly known as Gros Michel) from Uganda with similar data (Table 2). Paka and Terema were the only two representatives of the edible diploid group (AA) with fruit containing an average of 8.3 and 8.1 mg/kg DW of iron and zinc, respectively (Figure 2C,D). In the AAB and ABB groups, the cultivars with the highest iron concentrations, Gonja Nakatansese and Kivuvu, respectively, were from Uganda (Table 2) while the Australian sets averaged at 7.8 and 8.4 mg/kg, respectively

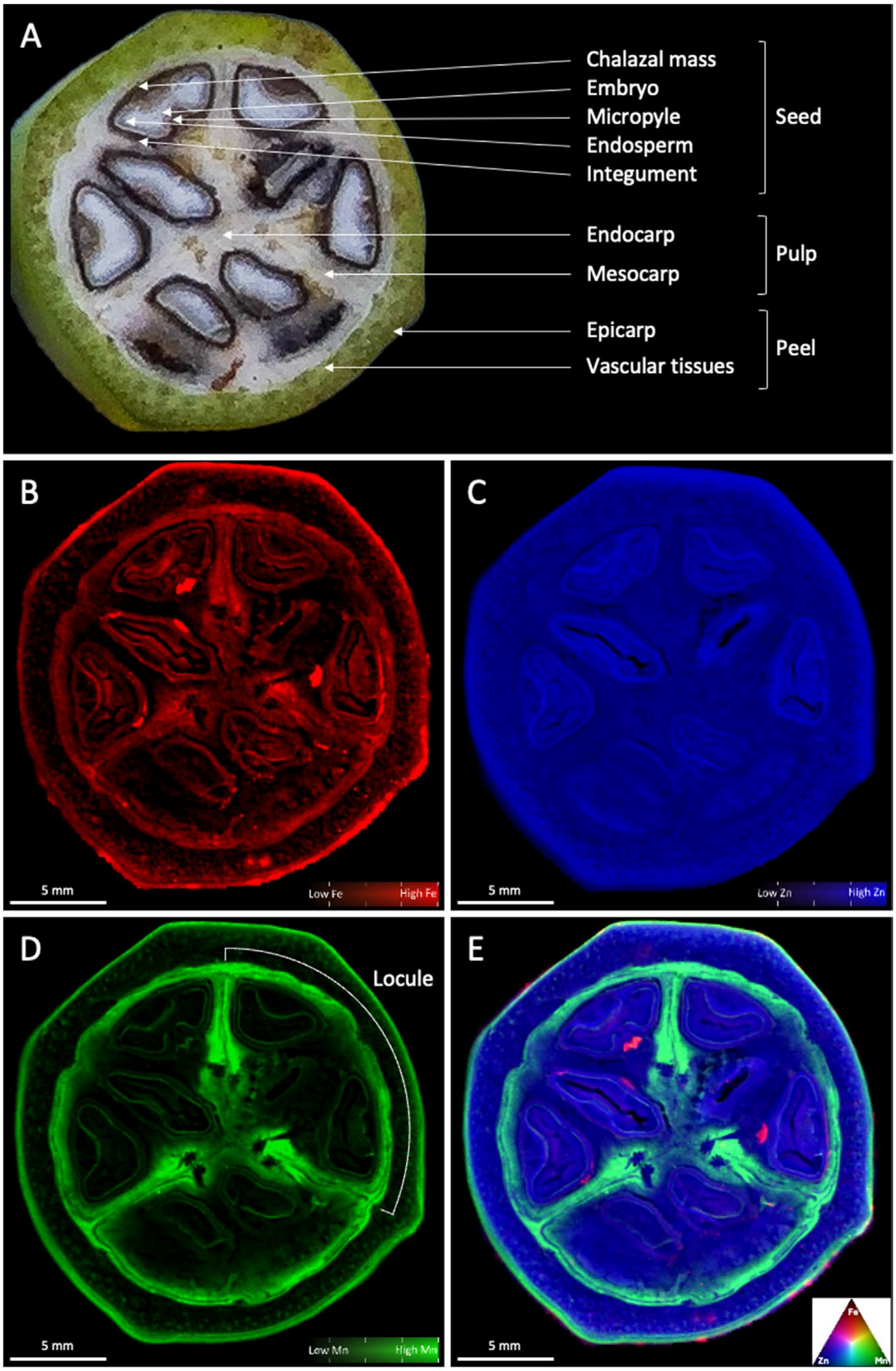

FIGURE 3 | X-ray fluorescence spectroscopy (µ-XRF) elemental mapping of a *M. acuminata* ssp. *zebrina* banana fruit cross section. (A) Fruit anatomy, (B) iron distribution, (C) zinc distribution, (D) manganese distribution and (E) composite image of iron, zinc, and manganese distribution. The color scale bar represents different elemental concentrations, with intensity corresponding to the lowest and highest concentrations, respectively. The color scale triangle represents different elemental concentrations, with red for iron, blue for zinc and green for manganese. McGahan (1961) was used to identify different parts of the banana fruit tissues. N.b. the micropyle also includes the micropylar plug and hilum.

(Table 2 and Figure 2C). Finally, the EAHB group for which large quantities of fruit pulp samples had been collected from various farms in Uganda averaged at 10.7 and 7.7 mg/kg of iron and zinc (Table 2).

Analysis of peel iron concentrations revealed that, when averaged as groups, the ABB followed by the wild cultivars generally accumulated higher concentrations in this tissue than the rest of the germplasm, with AAA cultivars accumulating the least. However, a Kruskal–Wallis H test revealed that none of these differences were significant ($p > 0.05$) except for the comparison between the peel of the ABB and AAA cultivars (Figure S4A). Similarly, no significant differences were observed in peel zinc concentration across the groups. The average peel zinc concentration ranged from 35.0 to 40.9 mg/kg DW and did not vary significantly between genome groups ($p > 0.05$) (Figure S4B).

There have been several studies in biofortified and conventionally bred wheat (Fan et al. 2008; Garvin et al. 2006) and rice (Goloran et al. 2019; Moreno-Moyano et al. 2016; Impa et al. 2013) reporting a decline in yield as dry matter production increases. This phenomenon is often referred to as the "dilution effect," and is likely driven by crucial source/sink dynamics within the plant (Moreno-Moyano et al. 2016). Pearson's correlation and correlograms were used to better understand how iron and zinc in banana fruit could potentially influence fruit size and ultimately yield (Figure 4). In comparisons across all cultivars analyzed, the concentration of iron in the pulp was significantly positively correlated to that of zinc ($r = 0.75$, $p < 0.01$) (Figure 4A). This positive correlation was observed within all genotypes tested but was only significant for the Fe'i ($r = 0.87$, $p < 0.001$) cultivars (Figure 4F). Finger width and length were used together as an indicator of bunch weight with both these attributes significantly positively correlated to one another across all cultivars ($r = 0.71$, $p < 0.01$) and with varying degrees of strength and significance for each genome group (Figure 4). In general, both metrics correlated negatively with the content of iron and zinc throughout the fruit (pulp and peel) although only pulp iron seems to have a significant influence (Figure 4A). These observations were not reflected at the genotype level where peel iron and zinc content seem to play a much stronger negative influence on the size of the fruit especially in the AA, Fe'i and wild cultivars (Figure 4B–G). The "dilution effect" may explain the reduced iron concentrations measured across all edible banana cultivars. Like many other crops, it is likely that centuries of human-driven selective pressure for higher yields in banana have come at the expense of nutrient density.

3.3 | Distinct Mineral Profiles in Wild and Fe'i Bananas Highlight Potential for Better Nutrient Biofortification

To investigate whether higher nutrient loading existed in the Fe'i and wild banana cultivars, nine essential minerals measured in the pulp of all the cultivars were subjected to principal component analysis (PCA). The PCA biplot accounted for 55.4% of the total variation within the population (Figure 5A) with cultivars grouping and separating into three main clusters, the wild diploid, the Fe'i and the remainder of the edible cultivars (AA, AAA, AAB, and ABB).

Mineral concentrations were positively correlated with either the wild or Fe'i cultivars indicating unique mineral concentration profiles (ionomes) within these groups. Specifically, iron, zinc, calcium, magnesium, sodium, and manganese were strongly associated with the wild cultivars and negatively correlated with finger length and width. In contrast, copper, sulphur, phosphorus, and potassium as well as fruit size showed a stronger association with the Fe'i group (Figure 5A). The edible AA, AAA, AAB, and ABB cultivars negatively correlated with all pulp mineral concentrations but positively correlated with the size of the fruit (Figure 5A). This analysis suggests that wild diploids and Fe'i cultivars are differentiated by distinct ionomes with a strong influence on fruit size. This could be attributed to the enhanced storage sink strength reported in Fe'i bananas (Buah et al. 2016) compared to their parthenocarpic triploid A and/or B genome counterparts, possibly owing to their unique T genome. These outcomes support the possibility of enhancing the nutrient profile of bananas through biofortification by incorporating iron homeostasis genes from either the Fe'i cultivars or fertile diploids. Nonetheless, the intricate interplay of metal homeostasis in plants suggests that complex, multifactorial

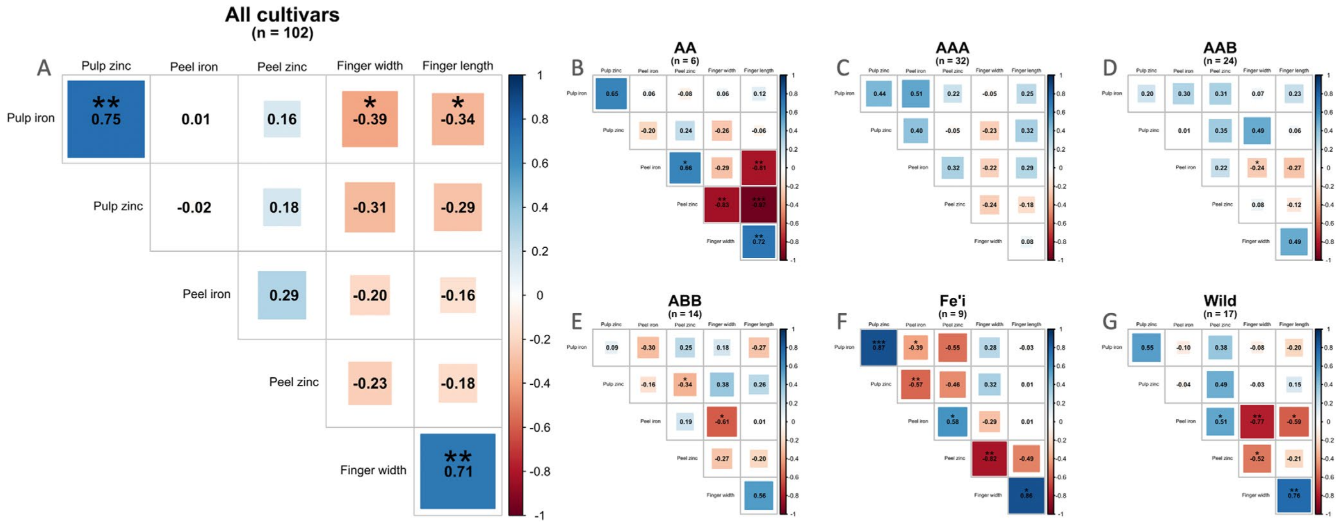

FIGURE 4 | Pearson's correlation coefficient matrix (correlogram) comparing paired covariates measured in different *Musa* spp. Measurements, comprising of pulp and peel iron and zinc concentrations, finger width, and finger length from (A) all cultivars screened, (B) AA cultivars, (C) AAA cultivars, (D) AAB cultivars, (E) ABB cultivars, (F) Fe'i cultivars, and (G) wild cultivars were compared to one another. Paired covariates Pearson correlation coefficient (r) is represented by (1) squares the size of which depict the strength of the correlation (coefficient value has been included in box) and (2) a colour scale for which positive correlations are blue while negative correlations are red. Statistical significance of p values are denoted as following * < 0.05, ** < 0.01, *** < 0.001. n, number of biological replicates.

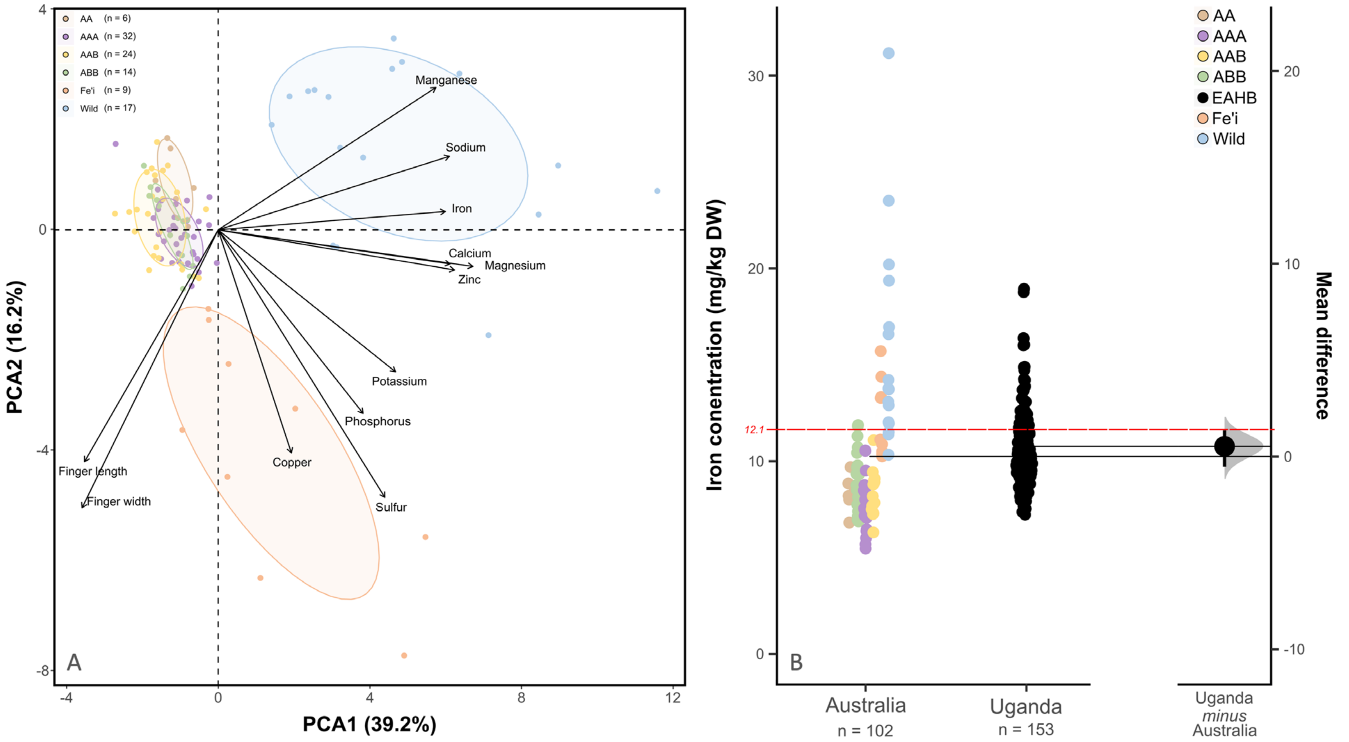

FIGURE 5 | Comparison of fruit micronutrients across different *Musa* genomes. (A) PCA biplot of pulp elemental profiles from *Musa* cultivars. Confidence ellipses ($p = 0.5$) indicate the true population mean of the bivariate distribution for the different banana populations. Eigen vector arrows represent the variable correlation plot. (B) Fruit pulp iron concentration in Australian grown cultivars compared to Ugandan grown EAHB cultivars. Gardner–Altman estimation statistics plots comparing fruit iron concentration from populations of Australian grown cultivars versus Ugandan grown EAHB cultivars. Each dot is a biological replicate from the respective cultivar. Dashed line represents the upper bounds of the bias-corrected accelerated confidence interval for the pulp iron concentration in Ugandan grown EAHB cultivars. DW, dry weight; *n*, number of biological replicates.

responses might accompany the increase in mineral concentrations from the expression of new genes (Briat et al. 2015; Antosiewicz et al. 2014). Of particular importance are possible yield constraints that could emerge in transgenic lines with enhanced iron concentrations.

3.4 | Comparison of Australian and EAHB *Musa* Cultivars

Estimation statistics were used to determine which cultivars grown in Australia had significantly higher fruit iron concentrations than EAHBs cultivated in Uganda. A bootstrapped Gardner–Altman plot was used to generate estimation statistics, and the upper bound of the bias-corrected and accelerated (BCa) confidence interval for pulp iron concentration in Ugandan-grown EAHB cultivars was calculated to be 12.1 mg/kg DW (Figure 5B). This upper BCa limit suggests that the true population mean for EAHB pulp iron concentration is unlikely to exceed this threshold. Cultivars with iron content above 12.1 mg/kg DW were therefore considered to have significantly higher pulp iron concentrations than the Ugandan-grown EAHBs. From this analysis, it was concluded that, on average, all wild-seeded cultivars and three Fe'i cultivars exhibited significantly higher pulp iron concentrations compared to most EAHBs.

3.5 | Identification and Diversity of Iron Homeostasis Genes in *Musa*

The molecular characterization of key genes involved in iron uptake, translocation, remobilization, sequestration, and storage has been largely overlooked in *Musa*. As an initial step towards addressing this issue and identifying potential targets for future exploitation, a systematic identification of genes associated with these processes was conducted initially focusing on the double haploid (AA) reference genome of *M. acuminata* ssp. *malaccensis* var. Pahang (DHP). The analysis was subsequently extended to four *Musa* species namely, Cavendish cv. Baxijiao (Cav, as a triploid representative of the acuminata genomes group 'A'), *M. balbisiana* var. Pisang Klutuk Wulung (PKW, as a diploid representative of the balbisiana genomes group "B"), and *M. troglodytarum* cv. Karat and Utafan (Kar and Uta, as triploid and diploid representatives of the troglodytarum genome group "T," respectively). Orthologous sequences were similarly identified from two *Musa* close relative species, *Ensete ventricosum* (Ev) and *E. glaucum* (Eg) to be use as outgroups in subsequent phylogenetic analysis (Table S5). In DHP, the sequences of 37 iron homeostasis genes were identified and their chromosomal positions recorded (Figure 6A and Table S4). Across the seven cultivars, a similar number of orthologous sequences were identified, with few exceptions (Table S4), yielding a total of 186 unique

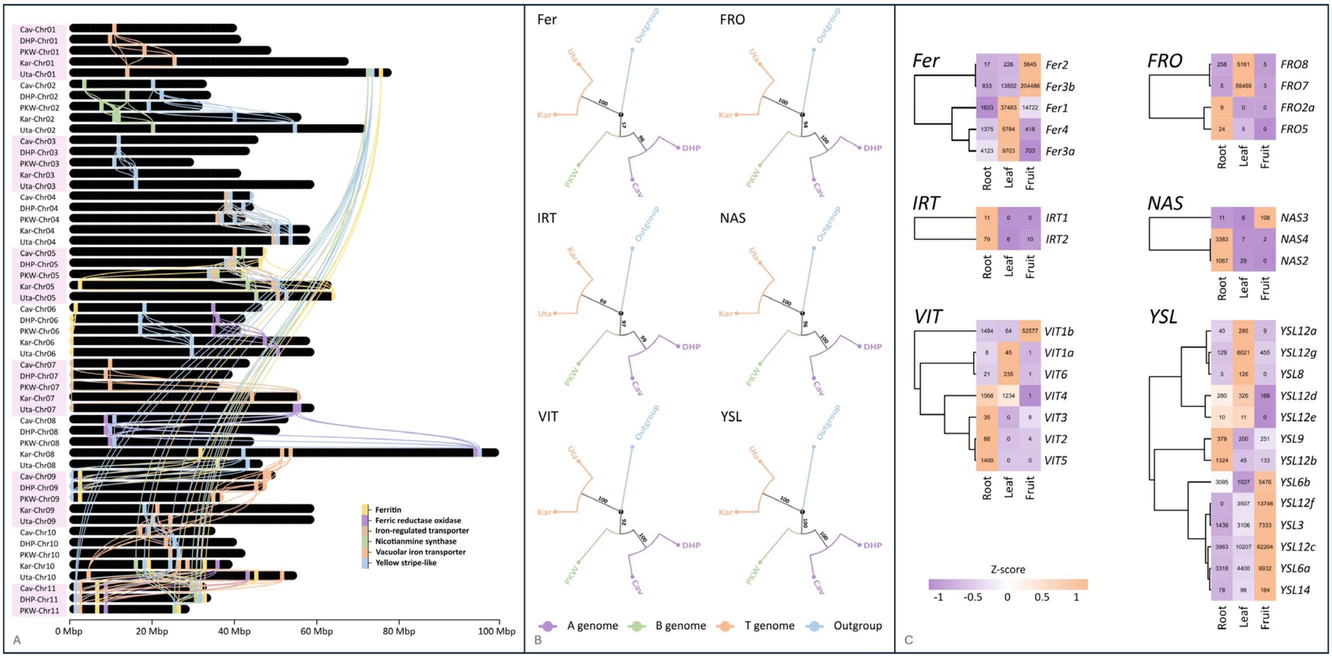

FIGURE 6 | (A) Chromosomal location of each identified iron homeostasis gene in Cavendish (Cav), DH-Pahang (DHP), Pisang Klutuk Wulung (PKW), Karat (Kar) and Utafan (Uta). Chr, chromosome; and Mbp, megabasepair. (B) Phylogenetic analysis of the iron homeostasis protein families found in *Musa* species. Fer, ferritin; FRO, ferric reductase oxidase; IRT, iron-regulated transporter; NAS, nicotianamine synthase; VIT, vacuolar iron transporter and YSL, yellow stripe-like. Trees were rooted using selected concatenated sequences from both the *Ensete ventricosum* and *E. glaucum* assemblies (outgroup). Cav, Cavendish; DHP, DH Pahang; PKW, Pisang Klutuk Wulung; Kar, Karat and Uta, Utafan. Nodes of the tree have their associated bootstrap values included. (C) Differential expression analysis of iron homeostasis genes in the fruit, leaves, and roots of wild-type Cavendish (cv. Grande Naine) banana. Fer, ferritin; FRO, ferric reductase oxidase; IRT, iron-regulated transporter; NAS, nicotianamine synthase; VIT, vacuolar iron transporter and YSL, yellow stripe-like. Data analyzed from three leaf, root and fruit biological replicates. Heat map constructed using relative expression values across the entire concatenated transcriptome and hierarchical clustering set to three clusters to identify genes within each tissue type. Estimated raw read counts aligning to each gene of interest is displayed within each box. Colours represent *Z*-scores that show how many standard deviations the given value is above or below the mean of all genes expressed in the transcriptome.

gene sequences from *Musa* and 75 from *Ensete*. In *Musa*, 14 sequences contained multiple stop codons or had less than 70% pairwise identity to their DHP orthologue, with 12 of these found in the Fe'i assemblies (Table S4). Consequently, these assemblies showed the highest frequency of "nonfunctional" proteins, likely reflecting limitations in using error-prone PacBio long reads and highlighting the need for resequencing efforts (Mitsuhashi et al. 2019; Weirather et al. 2017; Rhoads and Au 2015). Conversely, whole-genome duplication (WGD) events that occurred in bananas (D'Hont et al. 2012) tend to be unstable and progress towards a diploid state through structural rearrangements and genome downsizing, including the loss of duplicated genes following these events (Wendel 2015). This fragmentation involving the removal of duplicated and functionally redundant genes by accumulation of mutations could have played a major part in the evolutions of the Fe'i group. WGDs are a particularly predominant evolutionary phenomena in plants (Van de Peer et al. 2017) with gene duplication being understood as a rich source for phenotypic novelties (Flagel and Wendel 2009).

Whereas most species exhibited a comparable number of orthologues to DHP, however the diploid Fe'i Uta had two gene deletions (*VIT1a* and *VIT4*), potentially indicating that these paralogues had become functionally redundant and had progressively been removed from this genome. On the other hand, the duplications of *FRO2a* and *FRO5* in Uta and *VIT3* in Kar could have provided some evolutionary advantage. These events are consistent with forms of neofunctionalization (i.e., functional divergence of gene copies) or subfunctionalization (space-temporal repartition of the gene function) which could confer evolutionary advantages (Cenci et al. 2019). Our analysis showed that many of the gene families studied had a higher number of gene members than previously reported from other plant species or at the very least showcased evidence of gene duplications. This aligns with reports of a substantial presence of duplicated genes in the *Musa* genome, particularly within well-studied gene families, as compared to other species (Cenci and Rouard 2017; Cenci et al. 2014; D'Hont et al. 2012). Furthermore, it is consistent with the reported three WGDs that occurred independently of other monocot lineages during the evolutionary history of banana, resulting in a complex paleopolyploid genome with multiple paralogues (D'Hont et al. 2012).

While expansions of most iron homeostasis gene families were observed, there were some exceptions. For example, only four gene orthologues of *NAS* were found in banana, which is the same as in Arabidopsis (Klatte et al. 2009; Bauer et al. 2004) and only one more than reported from rice (Johnson et al. 2011). Only two *IRT* genes were identified across the broader *Musa* genomes in this study, which is very similar to reported studies from both rice (Ishimaru et al. 2007; Bughio et al. 2002) and Arabidopsis

(Vert et al. 2002; Eide et al. 1996) where they have been well-characterized. Eight *FRO* genes have been documented in Arabidopsis (Mukherjee et al. 2006) while only two have been identified in rice. However, neither of these exhibited significant Fe^{3+}-chelate reductase activity when tested in yeast, possibly reflecting a characteristic of Strategy II plants (Li et al. 2019). An extensive examination of the *Arachis hypogaea* (peanut) genome revealed that *AhFRO* underwent WGD/segmental duplications, resulting in the expansion of the *AhFRO* gene family to nine genes, five of which are duplications of *AhFRO2* (Guan et al. 2024). In all banana genomes investigated, *FRO2* was found duplicated at least once on the same chromosome, an observation that was also seen in both *Ensete* species considered distant relatives of *Musa*. Except for Uta, which underwent an additional duplication event of *FRO2a* and *FRO5*, five *FRO* genes were identified among the analyzed *Musa* species. These duplications may be attributed to the allopolyploid nature of *Musa* species, although there may be evolutionary advantages in avoiding gene loss, particularly since banana is a strategy I plant (Römheld 1987b) that relies on *FRO2* for efficient iron uptake from the soil. The duplication events observed in the banana ferritin gene family, specifically *Fer3*, led to the identification of five ferritin genes, surpassing those found in Arabidopsis by one (Petit et al. 2001) and rice by three (Nguyen et al. 2022; Gross et al. 2003). Similarly, *Musa* species exhibited duplication events in the *VIT* gene family, notably on Chromosome 11, and a duplication of *VIT1* on Chromosomes 7 and 9. The Kar cultivar was also the only *Musa* species to have an additional *VIT3* gene found on the same chromosome. A study into the molecular evolution of *VIT* family genes revealed a wide range of *VIT* gene numbers in plants, ranging from 2 to 21, with instances of gain and loss (Cao 2019). Moreover, hexaploid wheat contains 31 vacuolar iron transporter-like (*VTL*) genes (Sharma et al. 2020), while Arabidopsis possesses one *VIT* gene (Kim et al. 2006) and two known *VTL* genes (Gollhofer et al. 2014). In contrast, rice harbors only two *VIT* genes (Zhang et al. 2012). Considering the intricate nature of the *VIT* gene family and the significant sequence homology shared between *VIT* and *VTL* genes (Gollhofer et al. 2014), it is plausible that some of the identified *VIT* genes in *Musa* are, in fact, *VTL* genes or simply duplications of other *VIT* genes. Therefore, further investigation into the *Musa VIT* gene family is warranted.

The *YSL* gene family shows significant diversity across plant species while maintaining a highly conserved transmembrane protein structure (Chowdhury et al. 2022). Arabidopsis possesses only eight YSL protein encoding genes (Hofstetter et al. 2013), whereas 13 were found in the *Musa* species examined in this study. Monocot plants, in general, have experienced common duplication events in the *YSL* gene family, resulting in an expansion (Chowdhury et al. 2022). For instance, rice (Aoyama et al. 2009; Koike et al. 2004) and maize (Song et al. 2024) express 18 and 19 different YSL transporters, respectively. These duplications are thought to play a crucial role in the functional diversification of the *YSL* gene family by altering spatial and temporal gene expression patterns and in part explain the high number of *YSL* genes found in banana (Chowdhury et al. 2022).

Overall, duplications of key genes in the Fer, FRO, VIT, and YSL protein families were observed in all *Musa* species investigated, with the Fe'i cultivars exhibiting the highest number of duplication events. These findings imply a concerted effort in *Musa* evolution to retain genes crucial for iron acquisition, transport, and sequestration. Interestingly, the T genome-containing banana cultivars undeniably demonstrated enhanced efficiency in these biological processes compared to the more common and commercially prevalent A and B genome-containing counterparts as evidenced by the observed elevated iron content in the fruit of the distinct Fe'i species.

3.6 | Phylogenetic Analyses of Iron Homeostasis Genes in *Musa*

Phylogenetic analysis incorporating sequences from wild relatives can offer valuable insights into the evolutionary relationships among the studied taxa, shedding light on their genetic divergence, phylogenetic history, and acquisition of specific unique traits or adaptations (Brozynska et al. 2016). Therefore, phylogenetic analyses were conducted aiming at understanding how iron-regulating proteins may have evolved from ancestral seeded diploids (AA and BB) and Fe'i cultivars, and how these genomes relate to modern parthenocarpic triploid cultivars like the Cavendish. Identified gene sequences were translated into proteins, and for duplicated events, the sequence with the highest pairwise identity to the DHP reference was selected for phylogenetic analysis (Table S4). These proteins were retained for phylogenetic completeness. Orthologous iron homeostasis proteins from Ev and Eg were used as outgroups, substituting Ev proteins with Eg where multiple stop codons or low identity occurred (Table S5).

For the analysis, protein family (Figure 6B) as well as individual protein comparisons (Figures S6–S9) were made. The clustering pattern observed was the same across all protein families, with sequences derived from the two T genomes containing cultivars Kar and Uta consistently forming a separate clade more closely associated to the *Ensete* outgroups than the other cultivars and consistently exhibiting greater evolutionary divergence from A genome-containing cultivars (Cav and DHP) compared with the B genome-containing PKW cultivar (Figure 6B). In all but two instances, these nodes were supported by bootstrap values exceeding 92%, with one of these exceptions located within the IRT family tree, which contains only two family members with ambiguous Fe'i sequences. This clustering pattern was also observed in 59.5% (22/37) of all individual proteins investigated (Figures S5–S9) and fell to 37.5% for the VIT family. In rare instances where proteins from the T and A genome cultivars clustered closer together, such as with FRO2b (Figure S6), NAS2 (Figure S7B), VIT2 and VIT4 (Figure S8) as well as a YSL6a, YSL8, and YSL12e (Figure S9), the analysis contained nonfunctional proteins and/or exhibited low bootstrapping values.

This analysis highlights conserved and divergent features reflecting adaptation mechanisms specific to iron metabolism within the *Musa* genus. Specifically, it again suggests distinct and divergent proteomes for iron uptake and regulation in Fe'i (T) and Cavendish (A) bananas. In light of this, key genes involved in iron homeostasis in Fe'i bananas should be functionally validated with a view to exploiting them as candidate cisgenes for iron biofortification. To facilitate this, a differential expression analysis of all previously identified genes was conducted on root, leaf, and fruit tissues of the Cavendish banana cultivars “Grande Naine” and “Williams.”

3.7 | Differential Expression of Iron Homeostasis Genes in Cavendish

Differential gene expression and the resulting phenotypic variations within *Musa* species can often be attributed to their distinct sub-genomes. For example, B genome cultivars have shown upregulation in genes associated with flavonoid biosynthesis, fatty acid metabolism, as well as amino and nucleotide sugar metabolism (Cenci et al. 2019). Additionally, multiple chromosome rearrangements and sequence variations in the triploid T genome of Kar and the diploid T genome of Uta have led to distinctive fruit traits linked to enhanced nutritional quality, including nonclimacteric ripening and increased concentrations of carotenoids, riboflavin, flavonoids, and free galactose (Zhou et al. 2024; Li et al. 2022).

Our approach began with investigating gene expression in Cavendish under iron-sufficient conditions to identify baseline bottlenecks. To achieve this, RNA-seq datasets from Cavendish root, leaf, and fruit tissues were systematically mapped to 37 iron homeostasis genes identified from the DHP assembly. Relative expression patterns were compared across these tissues (Figure 6C) to facilitate the selection of candidate genes for biofortification and to enhance our understanding of the spatial expression patterns of these genes within the plant.

Genes encoding ferritin (*Fer*) were found to be mainly expressed in leaves and fruit, with *Fer2* and *Fer3b* most strongly differentially expressed in the fruit, while *Fer1*, *Fer4*, and *Fer3a* had higher differential expression in leaves (Figure 6C). Among these, *Fer3b*, a duplicated gene, displayed the highest overall expression levels in fruit, which were over five-fold higher than the next highest *Fer* gene (*Fer1* in leaf). *Fer3b* was also found to be substantially expressed in the leaves (13,502 normalized read counts) when compared to *Fer1*, which was the highest leaf-expressed gene with 37,483 normalized read counts. *Fer3* is believed to fulfil a role akin to the Arabidopsis *AtFer2* gene, which is known for storing iron specifically in seeds (Petit et al. 2001) and has emerged as a strong candidate gene for iron storage in bananas, likely playing a pivotal role not only during fruit maturation but also at other developmental stages.

The chloroplastic ferric reductase oxidase genes, *FRO7* and *FRO8*, had strong differential expression in leaf tissues compared to both root and fruit tissues, where the expression of both genes was minimal (Figure 6C). This pattern aligns with findings in Arabidopsis, where *AtFRO7* and *AtFRO8* are predominantly expressed in photosynthetic tissues and shoots, respectively (Mukherjee et al. 2006). Low expression levels of *FRO2a* and *FRO5* but also *IRT1* and *IRT2* were observed in all banana tissues, with the highest expression detected in root tissues (Figure 6C). This expression pattern mirrors that of their respective Arabidopsis orthologues, *AtIRT1* (Vert et al. 2002), *AtIRT2* (Vert et al. 2009), *AtFRO2*, and *AtFRO5* (Mukherjee et al. 2006), which are known to express in roots. Low expression of these genes was expected under iron-sufficient conditions, indicating sufficient iron absorption from the soil in mature plants. However, considering the importance of these genes for iron uptake in nongraminaceous monocotyledonous plants such as banana, strong upregulation would be expected under iron-deficient conditions, as is the case for both Arabidopsis (Vert et al. 2002) and rice (Lee and An 2009).

The identified *NAS* genes appeared to be predominantly expressed in roots and at significantly higher levels compared with other tissues (Figure 6C). *NAS4* exhibited the highest overall expression, which was three-fold higher than the next highest gene, *NAS2*. *NAS3* was found to be the only *NAS* gene expressed in banana fruit, although its estimated read counts are consistent with low activity in this tissue (Figure 6C). As *NAS* expression was primarily restricted to the roots, nicotianamine (NA) synthesis likely occurs in banana roots, and then NA, presumably bound to iron, is transported to other parts of the plant as required. This localization pattern aligns with findings in rice, where NAS is predominantly localized to vesicles in iron-deficient root cells, enabling efficient NA synthesis and facilitating iron uptake and long-distance transport within the plant (Kobayashi and Nishizawa 2012). Similarly, in maize, both *ZmNAS1* and *ZmNAS2* are expressed in the cortex and stele of roots, while *ZmNAS3* is typically expressed in axillary meristems, leaf primordia, and mesophyll cells (Zhou et al. 2013). In banana, *NAS1* expression was undetectable, while *NAS3* was expressed exclusively in the fruit but at a low abundance. Given the extremely low amount of expression detected from these genes in the tissues tested, it is possible that a more specialized organ or tissue serves as the primary site of expression.

In general, the eight *VIT* genes identified had low expression in most tested tissues, except for *VIT1b* with fruit expression 40-fold higher than any other *VIT* gene across all tissues tested (Figure 6C). *VIT4* had measurable expression levels in the leaves (Figure 6C) while it also had comparable expression levels in root tissues similar to genes *VIT5* and *VIT1b*. The low expression of *VIT* genes in *Musa* may indicate that either (i) at the time of sampling the plant had already stored most of the iron it had absorbed or (ii) these duplicated genes have become redundant. The strong fruit expression of *VIT1b* suggests a similar role to *AtVIT1* which localizes specifically to the seed vacuoles of Arabidopsis (Kim et al. 2006). This expression pattern suggests that Cavendish *VIT4* may function similarly to the rice *OsVIT1* and *OsVIT2* genes, which are most active in flag leaves (Zhang et al. 2012). Further research is needed to explore this potential functional parallel in banana. The significant upregulation of *VIT1b* in the fruit and the lack of associated increase in iron storage in that tissue remain unexplained and also require investigation. From a biofortification perspective and with the current state of knowledge, *VIT1b* might not be the ideal candidate to increase fruit iron storage. In contrast, *VIT4* which showed moderate expression in banana leaves, a known site of iron accumulation, could be a more suitable candidate to increase fruit iron concentration if expressed in a fruit-specific manner.

YSL genes, the largest gene family analyzed in this study, exhibited the widest variation in gene expression across all three banana tissue types. This aligns with findings in maize, where *YSL* genes were shown to be expressed in multiple tissues (Song et al. 2024). In bananas, the highest overall *YSL* gene expression was observed in the fruit, likely influenced by its developmental stage during sampling. A clade consisting of six *YSL* genes was found to be differentially expressed in Cavendish fruit, with *YSL12c* having by far the strongest expression at more than 4.5-fold that of *YSL12f*, the next highly expressed gene in that clade (Figure 6C). Decreasing expression was then found in *YSL6a*, *YSL3*, *YSL6b*, and *YSL14*. Although the expression of *YSL14* was differentially favored toward the fruit, the estimated read counts in this tissue as well as the other two tissue types tested were indicative of very low expression. Interestingly, out of the six genes in that clade, all but one (*YSL6b*) had the same tissue expression profile with the lowest expression in root, followed by leaf and finally fruit. Two genes in the adjoining clade were differentially expressed in the roots, with *YSL12b* being the strongest expressor of the two. However, the most highly expressed genes in root tissues were *YSL12c*, *YSL6a*, and *YSL6b*. The three *YSL* genes with the strongest leaf expression were *YSL12c* followed by *YSL12g and YSL6a* (Figure 6C). Importantly, *YSL12c*, *YSL6a*, and *YSL3* showed high expression in all three tissues, suggesting their potential involvement in long-distance transport of divalent cations. This expression pattern indicates that these genes and those within the same clade may belong to Subgroup I *YSLs*, which are associated with long-distance iron transport. Of these, *YSL12c* exhibited the highest expression in the fruit, making it a promising candidate for future biofortification attempts. In maize, *ZmYSL3* and *ZmYSL11* are Subgroup I *YSLs*, while several other *YSLs* (*ZmYSL2*, *5*, *7*, *9*, and *12*) show relatively high expression in the embryo or endosperm (Song et al. 2024). In well-studied plants like Arabidopsis, rice, and maize, Subgroup II *YSLs* such as *AtYSL4* and *AtYSL6* (Divol et al. 2013), *OsYSL6* (Sasaki et al. 2011), *ZmYSL4* and *ZmYSL5* (Song et al. 2024), primarily regulate metal storage and detoxification rather than long-distance transport. Although the specific identity of these Subgroup II *YSL* genes in Cavendish bananas remains unclear, it is likely that those in the second clade (Figure 6C) may participate in localized metal detoxification and storage. These genes typically exhibit expression in only one specific tissue, such as *YSL12b*, which is predominantly expressed in the roots, or *YSL12g*, which is mainly expressed in the leaves. Possibly, the two clades identified in the YSL gene expression profiles may correspond to the distinct functional roles of the Subgroups I and II *YSL* genes in banana, thus explaining the observed overlapping expression patterns across different tissues. Elucidating the roles of these genes in bananas is vital for understanding the regulatory mechanisms governing this crucial gene family in a key food crop.

4 | Future Directions

This study sought to lay the groundwork for identifying and characterizing key iron homeostasis genes in *Musa*, aiming to pinpoint suitable cisgene candidates for biofortification purposes. By leveraging iron homeostasis genes sourced from cultivars with naturally high iron and zinc content, a tailored approach to enhancing the nutritional profile of bananas can be designed in the future. An important outcome from the germplasm screening is the superior nutrient accumulation capabilities of bananas belonging to the Fe'i group, and underscores the potential of these bananas as a valuable resource in biofortification efforts, a concept previously illustrated by Paul et al. (2017). In Fe'i bananas, both the ionome profiles of the pulp and the iron homeostasis proteins markedly differ from those of commercially cultivated banana cultivars. Consequently, conducting comprehensive gene expression studies on these bananas under iron-sufficient and -deficient conditions represents a natural progression for future research endeavours.

Author Contributions

The original idea was conceived by J.L.D., R.H., and J.-Y.P. Data analysis was carried out by T.C., Z.S., and J.-Y.P. Experiments were performed by T.C., A.P., J.D., Z.S., and M.M. The manuscript was written by T.C. and J.-Y.P., reviewed, discussed, and approved by all authors.

Acknowledgements

The Banana21 project is supported by the Bill & Melinda Gates Foundation and the Department for International Development (United Kingdom). Some of the data reported in this paper was generated at the Central Analytical Research Facility (CARF) operated by the Institute for Future Environments (IFE, QUT). Access to CARF is supported with funding from the Science and Engineering Faculty, QUT. The technical assistance of current and past members of the Banana Biotechnology Program within the Centre for Agriculture and the Bioeconomy, QUT, is gratefully acknowledged. Open access publishing facilitated by Queensland University of Technology, as part of the Wiley - Queensland University of Technology agreement via the Council of Australian University Librarians.

Conflicts of Interest

The authors declare no conflicts of interest.

Data Availability Statement

The data that support the findings of this study are available from the corresponding author upon reasonable request.

References

Andrews, S. 2010. "FastQC: A Quality Control Tool for High Throughput Sequence Data." Available online at: http://www.bioinformatics.babraham.ac.uk/projects/fastqc/

Antosiewicz, D. M., A. Barabasz, and O. Siemianowski. 2014. "Phenotypic and Molecular Consequences of Overexpression of Metal-Homeostasis Genes." *Frontiers in Plant Science* 5: 80.

Aoyama, T., T. Kobayashi, M. Takahashi, et al. 2009. "OsYSL18 is a Rice Iron(III)-Deoxymugineic Acid Transporter Specifically Expressed in Reproductive Organs and Phloem of Lamina Joints." *Plant Molecular Biology* 70: 681–692.

Aquino, C., L. Salomão, D. Siqueira, P. Cecon, and S. Ribeiro. 2014. "Mineral Content in the Pulp and Peel of Banana Cultivars." *Pesquisa Agropecuária Brasileira* 49: 546–553.

Arnaud, E., and J. P. Horry. 1997. *A Catalogue of Musa Germplasm: Papua New Guinea Collecting Missions 1988–1989*. International Plant Genetic Resources Institute.

Arosio, P., R. Ingrassia, and P. Cavadini. 2009. "Ferritins: A family of molecules for iron storage, antioxidation and more." *Biochimica et Biophysica Acta* 1790: 589–599.

Bauer, P., T. Thiel, M. Klatte, et al. 2004. "Analysis of Sequence, Map Position, and Gene Expression Reveals Conserved Essential Genes for Iron Uptake in Arabidopsis and Tomato." *Plant Physiology* 136: 4169–4183.

Beasley, J. T., J. P. Bonneau, J. T. Sánchez-Palacios, et al. 2019. "Metabolic Engineering of Bread Wheat Improves Grain Iron Concentration and Bioavailability." *Plant Biotechnology Journal* 17: 1514–1526.

Becker, D. K., B. Dugdale, M. K. Smith, R. M. Harding, and J. L. Dale. 2000. "Genetic Transformation of Cavendish Banana (*Musa* spp. AAA Group) cv 'Grand Nain' via Microprojectile Bombardment." *Plant Cell Reports* 19: 229–234.

Belser, C., F. C. Baurens, B. Noel, et al. 2021. "Telomere-To-Telomere Gapless Chromosomes of Banana Using Nanopore Sequencing." *Communications Biology* 4: 1047.

Bonneau, J., U. Baumann, J. Beasley, Y. Li, and A. A. T. Johnson. 2016. "Identification and Molecular Characterization of the Nicotianamine Synthase Gene Family in Bread Wheat." *Plant Biotechnology Journal* 14: 2228–2239.

Bouis, H. E., C. Hotz, B. McClafferty, J. V. Meenakshi, and W. H. Pfeiffer. 2011. "Biofortification: A New Tool to Reduce Micronutrient Malnutrition." *Food and Nutrition Bulletin* 32: S31–S40.

Bray, N. L., H. Pimentel, P. Melsted, and L. Pachter. 2016. "Near-Optimal Probabilistic RNA-Seq Quantification." *Nature Biotechnology* 34: 525–527.

Briat, J. F., C. Dubos, and F. Gaymard. 2015. "Iron Nutrition, Biomass Production, and Plant Product Quality." *Trends in Plant Science* 20: 33–40.

Briat, J.-F., I. Fobis-Loisy, N. Grignon, et al. 1995. "Cellular and Molecular Aspects of Iron Metabolism in Plants." *Biology of the Cell* 84: 69–81.

Brozynska, M., A. Furtado, and R. J. Henry. 2016. "Genomics of Crop Wild Relatives: Expanding the Gene Pool for Crop Improvement." *Plant Biotechnology Journal* 14: 1070–1085.

Buah, S., B. Mlalazi, H. Khanna, J. L. Dale, and C. L. Mortimer. 2016. "The Quest for Golden Bananas: Investigating Carotenoid Regulation in a Fe'i Group *Musa* Cultivar." *Journal of Agricultural and Food Chemistry* 64: 3176–3185.

Bughio, N., H. Yamaguchi, N. K. Nishizawa, H. Nakanishi, and S. Mori. 2002. "Cloning an Iron-Regulated Metal Transporter From Rice." *Journal of Experimental Botany* 53: 1677–1682.

Cao, J. 2019. "Molecular Evolution of the *Vacuolar Iron Transporter* (*VIT*) Family Genes in 14 Plant Species." *Genes (Basel)* 10: 144.

Cenci, A., V. Guignon, N. Roux, and M. Rouard. 2014. "Genomic Analysis of NAC Transcription Factors in Banana (*Musa acuminata*) and Definition of NAC Orthologous Groups for Monocots and Dicots." *Plant Molecular Biology* 85: 63–80.

Cenci, A., Y. Hueber, Y. Zorrilla-Fontanesi, et al. 2019. "Effect of Paleopolyploidy and Allopolyploidy on Gene Expression in Banana." *BMC Genomics* 20: 244.

Cenci, A., and M. Rouard. 2017. "Evolutionary Analyses of GRAS Transcription Factors in Angiosperms." *Frontiers in Plant Science* 8: 273.

Chowdhury, R., S. Nallusamy, V. Shanmugam, et al. 2022. "Genome-Wide Understanding of Evolutionary and Functional Relationships of Rice Yellow Stripe-Like (YSL) Transporter Family in Comparison With Other Plant Species." *Biologia* 77: 39–53.

Connorton, J. M., and J. Balk. 2019. "Iron Biofortification of Staple Crops: Lessons and Challenges in Plant Genetics." *Plant and Cell Physiology* 60: 1447–1456.

Connorton, J. M., E. R. Jones, I. Rodríguez-Ramiro, S. Fairweather-Tait, C. Uauy, and J. Balk. 2017. "Wheat Vacuolar Iron Transporter TaVIT2 Transports Fe and Mn and Is Effective for Biofortification." *Plant Physiology* 174: 2434–2444.

Daniells, J. W. 1986. "Banana Cultivars in Australia." *Queensland Agricultural Journal* 50: 24–26.

Daniells, J. W., and N. J. Bryde. 2001. "Banana Varieties: The ACIAR Years 1987–1996." In *Information Series QI01013*, edited by Queensland Department of Primary Industries. Queensland Department of Primary Industries.

Daniells, J. W., and S. Hamill. 2004. "Banana Varieties 1997–2002." In *Information Series QI04033*, edited by Queensland Department of Primary Industries and Fisheries. Queensland Department of Primary Industries and Fisheries.

Davey, M. W., I. Van den Bergh, R. Markham, R. Swennen, and J. Keulemans. 2009. "Genetic Variability in *Musa* Fruit Provitamin A Carotenoids, Lutein and Mineral Micronutrient Contents." *Food Chemistry* 115: 806–813.

Detzel, P., and S. Wieser. 2015. "Food Fortification for Addressing Iron Deficiency in Filipino Children: Benefits and Cost-Effectiveness." *Annals of Nutrition and Metabolism* 66, no. Suppl 2: 35–42.

D'Hont, A., F. Denoeud, J. M. Aury, et al. 2012. "The Banana (*Musa acuminata*) Genome and the Evolution of Monocotyledonous Plants." *Nature* 488: 213–219.

Divol, F., D. Couch, G. Conéjéro, H. Roschzttardtz, S. Mari, and C. Curie. 2013. "The Arabidopsis Yellow Striple Like 4 and 6 Transporters Control Iron Release From the Chloroplast." *Plant Cell* 25: 1040–1055.

Droc, G., D. Larivière, V. Guignon, et al. 2013. "The Banana Genome Hub." *Database: The Journal of Biological Databases and Curation* 2013: bat035.

Eide, D., M. Broderius, J. Fett, and M. L. Guerinot. 1996. "A Novel Iron-Regulated Metal Transporter From Plants Identified by Functional Expression in Yeast." *Proceedings of the National Academy of Sciences of the United States of America* 93: 5624–5628.

Englberger, L., W. Aalbersberg, P. Ravi, et al. 2003. "Further Analyses on Micronesian Banana, Taro, Breadfruit and Other Foods for Provitamin A Carotenoids and Minerals." *Journal of Food Composition and Analysis* 16: 219–236.

Fan, M. S., F. J. Zhao, S. J. Fairweather-Tait, P. R. Poulton, S. J. Dunham, and S. P. McGrath. 2008. "Evidence of Decreasing Mineral Density in Wheat Grain Over the Last 160 Years." *Journal of Trace Elements in Medicine and Biology* 22: 315–324.

Finkelstein, J. L., J. D. Haas, and S. Mehta. 2017. "Iron-Biofortified Staple Food Crops for Improving Iron Status: A Review of the Current Evidence." *Current Opinion in Biotechnology* 44: 138–145.

Flagel, L. E., and J. F. Wendel. 2009. "Gene Duplication and Evolutionary Novelty in Plants." *New Phytologist* 183: 557–564.

Fungo, R. 2010. "Potential of Bananas in Alleviating Micronutrient Deficiencies in the Great Lakes Region of East Africa." In: *African Crop Science Conference Proceedings*, 317–324.

Fungo, R., and M. Pillay. 2011. "β-Carotene Content of Selected Banana Genotypes From Uganda." *African Journal of Biotechnology* 10: 5423–5430.

García, O. P., M. Martınez, D. Romano, et al. 2015. "Iron Absorption in Raw and Cooked Bananas: A Field Study Using Stable Isotopes in Women." *Food & Nutrition Research* 59: 25976.

Garvin, D. F., R. M. Welch, and J. W. Finley. 2006. "Historical Shifts in the Seed Mineral Micronutrient Concentration of US Hard Red Winter Wheat Germplasm." *Journal of the Science of Food and Agriculture* 86: 2213–2220.

Gollhofer, J., R. Timofeev, P. Lan, W. Schmidt, and T. J. Buckhout. 2014. "Vacuolar-Iron-Transporter1-Like Proteins Mediate Iron Homeostasis in Arabidopsis." *PLoS One* 9: e110468.

Goloran, J. B., S. E. Johnson-Beebout, M. J. Morete, S. M. Impa, G. J. D. Kirk, and M. Wissuwa. 2019. "Grain Zn Concentrations and Yield of Zn-Biofortified Versus Zn-Efficient Rice Genotypes Under Contrasting Growth Conditions." *Field Crops Research* 234: 26–32.

Govindaraj, M., K. N. Rai, B. Cherian, W. H. Pfeiffer, A. Kanatti, and H. Shivade. 2019. "Breeding Biofortified Pearl Millet Varieties and Hybrids to Enhance Millet Markets for Human Nutrition." *Agriculture* 9: 106.

Gregorio, G. B., D. Senadhira, H. Htut, and R. D. Graham. 2000. "Breeding for Trace Mineral Density in Rice." *Food and Nutrition Bulletin* 21: 382–386.

Gross, J., R. J. Stein, A. G. Fett-Neto, and J. P. Fett. 2003. "Iron Homeostasis Related Genes in Rice." *Genetics and Molecular Biology* 26: 477–497.

Guan, J., Z. Zhang, and G. Shi. 2024. "Genome-Wide Identification of the *Ferric Chelate Reductase* (*FRO*) Gene Family in Peanut and Its Diploid Progenitors: Structure, Evolution, and Expression Profiles." *Plants* 13: 418.

Haas, J. D., J. L. Beard, L. E. Murray-Kolb, A. M. del Mundo, A. Felix, and G. B. Gregorio. 2005. "Iron-Biofortified Rice Improves the Iron Stores of Nonanemic Filipino Women." *Journal of Nutrition* 135: 2823–2830.

Haas, J. D., S. V. Luna, M. G. Lung'aho, et al. 2016. "Consuming Iron Biofortified Beans Increases Iron Status in Rwandan Women After 128 Days in a Randomized Controlled Feeding Trial." *Journal of Nutrition* 146: 1586–1592.

Hofstetter, S. S., A. Dudnik, H. Widmer, and R. Dudler. 2013. "Arabidopsis Yellow Stripe-Like (YSL7) and YSL8 Transporters Mediate Uptake of *Pseudomonas* Virulence Factor Syringolin A Into Plant Cells." *Molecular Plant-Microbe Interactions* 26: 1302–1311.

Impa, S. M., M. J. Morete, A. M. Ismail, R. Schulin, and S. E. Johnson-Beebout. 2013. "Zn Uptake, Translocation and Grain Zn Loading in Rice (*Oryza sativa* L.) Genotypes Selected for Zn Deficiency Tolerance and High Grain Zn." *Journal of Experimental Botany* 64: 2739–2751.

Ishimaru, Y., S. Kim, T. Tsukamoto, et al. 2007. "Mutational Reconstructed Ferric Chelate Reductase Confers Enhanced Tolerance in Rice to Iron Deficiency in Calcareous Soil." *Proceedings of the National Academy of Sciences of the United States of America* 104: 7373–7378.

Johnson, A. A., B. Kyriacou, D. L. Callahan, et al. 2011. "Constitutive Overexpression of the *OsNAS* Gene Family Reveals Single-Gene Strategies for Effective Iron- and Zinc-Biofortification of Rice Endosperm." *PLoS One* 6, no. 9: e24476.

Kalyaanamoorthy, S., B. Q. Minh, T. K. Wong, A. Von Haeseler, and L. S. Jermiin. 2017. "ModelFinder: Fast Model Selection for Accurate Phylogenetic Estimates." *Nature Methods* 14: 587–589.

Katsvairo, L. 2014. "Delivery of Iron Beans in Rwanda." In *Biofortification Progress Brief 33*. International Food Policy Research Institute (IFPRI).

Kawakami, Y., W. Gruissem, and N. K. Bhullar. 2022. "Novel Rice Iron Biofortification Approaches Using Expression of *ZmYS1* and *OsTOM1* Controlled by Tissue-Specific Promoters." *Journal of Experimental Botany* 73: 5440–5459.

Khanna, H., D. Becker, J. Kleidon, and J. Dale. 2004. "Centrifugation Assisted *Agrobacterium tumefaciens*-Mediated Transformation (CAAT) of Embryogenic Cell Suspensions of Banana (*Musa* spp. Cavendish AAA and Lady Finger AAB)." *Molecular Breeding* 14: 239–252.

Khanna, H. K., J. Y. Paul, R. M. Harding, M. B. Dickman, and J. L. Dale. 2007. "Inhibition of Agrobacterium-Induced Cell Death by Antiapoptotic Gene Expression Leads to Very High Transformation Efficiency of Banana." *Molecular Plant-Microbe Interactions* 20: 1048–1054.

Kim, S. A., T. Punshon, A. Lanzirotti, et al. 2006. "Localization of Iron in Arabidopsis Seed Requires the Vacuolar Membrane Transporter VIT1." *Science* 314: 1295–1298.

Klatte, M., M. Schuler, M. Wirtz, C. Fink-Straube, R. Hell, and P. Bauer. 2009. "The Analysis of Arabidopsis Nicotianamine Synthase Mutants Reveals Functions for Nicotianamine in Seed Iron Loading and Iron Deficiency Responses." *Plant Physiology* 150: 257–271.

Kobayashi, T., and N. K. Nishizawa. 2012. "Iron Uptake, Translocation, and Regulation in Higher Plants." *Annual Review of Plant Biology* 63: 131–152.

Koike, S., H. Inoue, D. Mizuno, et al. 2004. "*OsYSL2* Is a Rice Metal-Nicotianamine Transporter That Is Regulated by Iron and Expressed in the Phloem." *Plant Journal* 39: 415–424.

Kumar, S. B., S. R. Arnipalli, P. Mehta, S. Carrau, and O. Ziouzenkova. 2022. "Iron Deficiency Anemia: Efficacy and Limitations of Nutritional and Comprehensive Mitigation Strategies." *Nutrients* 14: 1–20.

Lee, S., and G. An. 2009. "Over-Expression of *OsIRT1* Leads to Increased Iron and Zinc Accumulations in Rice." *Plant, Cell & Environment* 32: 408–416.

Li, L., L. Ye, Q. Kong, and H. Shou. 2019. "A Vacuolar Membrane Ferric-Chelate Reductase, OsFRO1, Alleviates Fe Toxicity in Rice (*Oryza sativa* L.)." *Frontiers in Plant Science* 10: 700.

Li, Z., J. Wang, Y. Fu, et al. 2022. "The *Musa troglodytarum* L. Genome Provides Insights Into the Mechanism of Non-Climacteric Behaviour and Enrichment of Carotenoids." *BMC Biology* 20: 186.

Martin, G., F.-C. Baurens, G. Droc, et al. 2016. "Improvement of the Banana "*Musa acuminata*" Reference Sequence Using NGS Data and Semi-Automated Bioinformatics Methods." *BMC Genomics* 17: 243.

Matovu, M. 2016. "Molecular and Biochemical Characterisation of Transgenic Banana Lines Containing Iron Uptake and Storage Enhancing Genes." PhD thesis, Queensland University of Technology, Faculty of Science and Engineering, Brisbane.

McGahan, M. W. 1961. "Studies on the Seed of Banana. I. Anatomy of the Seed and Embryo of *Musa balbisiana*." *American Journal of Botany* 48: 230–238.

Minh, B. Q., H. A. Schmidt, O. Chernomor, et al. 2020. "IQ-TREE 2: New Models and Efficient Methods for Phylogenetic Inference in the Genomic Era." *Molecular Biology and Evolution* 37: 1530–1534.

Mitsuhashi, S., M. C. Frith, T. Mizuguchi, et al. 2019. "Tandem-Genotypes: Robust Detection of Tandem Repeat Expansions From Long DNA Reads." *Genome Biology* 20: 1–17.

Moreno-Moyano, L. T., J. P. Bonneau, J. T. Sánchez-Palacios, J. Tohme, and A. A. T. Johnson. 2016. "Association of Increased Grain Iron and Zinc Concentrations With Agro-Morphological Traits of Biofortified Rice." *Frontiers in Plant Science* 7: 1463.

Morrissey, J., and M. L. Guerinot. 2009. "Iron Uptake and Transport in Plants: The Good, the Bad, and the Ionome." *Chemical Reviews* 109: 4553–4567.

Mukherjee, I., N. H. Campbell, J. S. Ash, and E. L. Connolly. 2006. "Expression Profiling of the Arabidopsis Ferric Chelate Reductase (*FRO*) Gene Family Reveals Differential Regulation by Iron and Copper." *Planta* 223: 1178–1190.

Narayanan, N., G. Beyene, R. D. Chauhan, et al. 2019. "Biofortification of Field-Grown Cassava by Engineering Expression of an Iron Transporter and Ferritin." *Nature Biotechnology* 37: 144–151.

Narayanan, N., G. Beyene, R. D. Chauhan, et al. 2015. "Overexpression of Arabidopsis *VIT1* Increases Accumulation of Iron in Cassava Roots and Stems." *Plant Science* 240: 170–181.

National Health and Medical Research Council, Australian Government Department of Health and Ageing New Zealand Ministry of Health. 2006. *Nutrient Reference Values for Australia and New Zealand Including Recommended Dietary Intakes.* National Health and Medical Research Council.

Nguyen, N. K., J. Wang, D. Liu, B. K. Hwang, and N. S. Jwa. 2022. "Rice Iron Storage Protein Ferritin 2 (OsFER2) Positively Regulates Ferroptotic Cell Death and Defense Responses Against *Magnaporthe oryzae*." *Frontiers in Plant Science* 13: 1019669.

Paul, J. Y., H. Khanna, J. Kleidon, et al. 2017. “Golden Bananas in the Field: Elevated Fruit Pro-Vitamin A From the Expression of a Single Banana Transgene.” *Plant Biotechnology Journal* 15: 520–532.

Pepper, R. A., G. Perenlei, W. N. Martens, and S. J. Couperthwaite. 2021. “High Purity Alumina Synthesised From Iron Rich Clay Through a Novel and Selective Hybrid Ammonium Alum Process.” *Hydrometallurgy* 204: 1–9.

Perrier, X., C. Jenny, F. Bakry, et al. 2019. “East African Diploid and Triploid Bananas: A Genetic Complex Transported From South-East Asia.” *Annals of Botany* 123: 19–36.

Petit, J.-M., J.-F. Briat, and S. Lobréaux. 2001. “Structure and Differential Expression of the Four Members of the *Arabidopsis thaliana* Ferritin Gene Family.” *Biochemical Journal* 359: 575–582.

Pillay, M., and R. Fungo. 2016. “Diversity of Iron and Zinc Content in Bananas From East and Central Africa.” *HortScience* 51: 320–324.

Pompano, L. M., S. V. Luna, S. A. Udipi, P. S. Ghugre, E. M. Przybyszewski, and J. Haas. 2022. “Iron-Biofortified Pearl Millet Consumption Increases Physical Activity in Indian Adolescent Schoolchildren After a 6-Month Randomised Feeding Trial.” *British Journal of Nutrition* 127: 1018–1025.

Rhoads, A., and K. F. Au. 2015. “PacBio Sequencing and Its Applications.” *Genomics, Proteomics & Bioinformatics* 13: 278–289.

Robinson, N. J., C. M. Procter, E. L. Connolly, and M. L. Guerinot. 1999. “A Ferric-Chelate Reductase for Iron Uptake From Soils.” *Nature* 397: 694–697.

Römheld, V. 1987a. “Different Strategies for Iron Acquisition in Higher Plants.” *Physiologia Plantarum* 70: 231–234.

Römheld, V. 1987b. “Existence of Two Different Strategies for the Acquisition of Iron in Higher Plants.” In *Iron Transport in Microbes, Plants and Animals*, edited by D. V. D. H. Gunther Winkelmann and J. B. Neilands, 353–374. VCH.

Sánchez, E., M. L. García-Bañuelos, and J. P. Sida-Arreola. 2012. “Biofortification – Promising Approach to Increasing the Content of Iron and Zinc in Staple Food Crops.” *Journal of Elementology* 19: 865–888.

Sasaki, A., N. Yamaji, J. Xia, and J. F. Ma. 2011. “OsYSL6 Is Involved in the Detoxification of Excess Manganese in Rice.” *Plant Physiology* 157: 1832–1840.

Sharma, S., G. Kaur, A. Kumar, et al. 2020. “Gene Expression Pattern of Vacuolar-Iron Transporter-Like (VTL) Genes in Hexaploid Wheat During Metal Stress.” *Plants* 9: 229.

Shojima, S., N. K. Nishizawa, S. Fushiya, S. Nozoe, T. Irifune, and S. Mori. 1990. “Biosynthesis of Phytosiderophores: *In Vitro* Biosynthesis of 2′-Deoxymugineic Acid From L-Methionine and Nicotianamine.” *Plant Physiology* 93: 1497–1503.

Shumate, A., and S. L. Salzberg. 2021. “Liftoff: Accurate Mapping of Gene Annotations.” *Bioinformatics* 37: 1639–1643.

Smith, M. K., J. W. Daniells, D. Peasley, et al. 2018. “Field Evaluation of Six Gros Michel Banana Accessions (*Musa* spp., AAA Group) for Agronomic Performance, Resistance to Fusarium Wilt Race 1 and Yellow Sigatoka.” *Crop Protection* 113: 84–89.

Song, Z., S. Li, Y. Li, et al. 2024. “Identification and Characterization of Yellow Stripe-Like Genes in Maize Suggest Their Roles in the Uptake and Transport of Zinc and Iron.” *BMC Plant Biology* 24: 3.

Takahashi, M., Y. Terada, I. Nakai, et al. 2003. “Role of Nicotianamine in the Intracellular Delivery of Metals and Plant Reproductive Development.” *Plant Cell* 15: 1263–1280.

Tauris, B., S. Borg, P. L. Gregersen, and P. B. Holm. 2009. “A Roadmap for Zinc Trafficking in the Developing Barley Grain Based on Laser Capture Microdissection and Gene Expression Profiling.” *Journal of Experimental Botany* 60: 1333–1347.

Taylor, N. J., N. Narayanan, G. Beyene, et al. 2016. “Iron and Zinc Biofortification of Cassava Storage Roots to Nutritionally Significant Levels.” *In Vitro Cellular & Developmental Biology* 52: S38–S39.

Theil, E. C. 2003. “Ferritin: At the Crossroads of Iron and Oxygen Metabolism.” *Journal of Nutrition* 133: 1549S–1553S.

Theil, E. C., J. W. Burton, and J. L. Beard. 1997. “A Sustainable Solution for Dietary Iron Deficiency Through Plant Biotechnology and Breeding to Increase Seed Ferritin Control.” *European Journal of Clinical Nutrition* 51, no. Suppl 4: S28–S31.

Thompson, J. D., D. G. Higgins, and T. J. Gibson. 1994. “CLUSTAL W: Improving the Sensitivity of Progressive Multiple Sequence Alignment Through Sequence Weighting, Position-Specific Gap Penalties and Weight Matrix Choice.” *Nucleic Acids Research* 22: 4673–4680.

Thomson, L. A., J.-F. Butaud, J. Daniells, et al. 2022. “The Origins and Dispersal Throughout the Pacific Islands of Fehi Bananas (*Musa* Series *Australimusa*).” *Journal of the Polynesian Society* 131: 289–335.

UBOS. 2017. “Uganda Demographic and Health Survey 2016: Key Indicators Report.” Kampala, Uganda; UBOS, and Rockville, Maryland USA: UBOS and ICF Uganda Bureau of Statistics.

USDA, AMS, FVP, and SCI. 2001. “Banana Ripening Guide.” (US Department of Agriculture. ed). California.

Van de Peer, Y., E. Mizrachi, and K. Marchal. 2017. “The Evolutionary Significance of Polyploidy.” *Nature Reviews Genetics* 18: 411–424.

Vasconcelos, M. W., W. Gruissem, and N. K. Bhullar. 2017. “Iron Biofortification in the 21st Century: Setting Realistic Targets, Overcoming Obstacles, and New Strategies for Healthy Nutrition.” *Current Opinion in Plant Biology* 44: 8–15.

Vert, G., M. Barberon, E. Zelazny, M. Séguéla, J. F. Briat, and C. Curie. 2009. “Arabidopsis IRT2 Cooperates With the High-Affinity Iron Uptake System to Maintain Iron Homeostasis in Root Epidermal Cells.” *Planta* 229: 1171–1179.

Vert, G., N. Grotz, F. Dédaldéchamp, et al. 2002. “IRT1, an Arabidopsis Transporter Essential for Iron Uptake From the Soil and for Plant Growth.” *Plant Cell* 14: 1223–1233.

Weirather, J. L., M. de Cesare, Y. Wang, et al. 2017. “Comprehensive Comparison of Pacific Biosciences and Oxford Nanopore Technologies and Their Applications to Transcriptome Analysis.” *F1000Research* 6: 100.

Wendel, J. F. 2015. “The Wondrous Cycles of Polyploidy in Plants.” *American Journal of Botany* 102: 1753–1756.

Wheal, M. S., T. O. Fowles, and L. T. Palmer. 2011. “A Cost-Effective Acid Digestion Method Using Closed Polypropylene Tubes for Inductively Coupled Plasma Optical Emission Spectrometry (ICP-OES) Analysis of Plant Essential Elements.” *Analytical Methods* 3: 2854–2863.

White, P. J., and M. R. Broadley. 2009. “Biofortification of Crops With Seven Mineral Elements Often Lacking in Human Diets – Iron, Zinc, Copper, Calcium, Magnesium, Selenium and Iodine.” *New Phytologist* 182: 49–84.

Wu, Q., C. Liu, Z. Wang, et al. 2022. “Zinc Regulation of Iron Uptake and Translocation in Rice (*Oryza sativa* L.): Implication From Stable Iron Isotopes and Transporter Genes.” *Environmental Pollution* 297: 118818.

Yadav, K., P. Patel, A. K. Srivastava, and T. R. Ganapathi. 2017. “Overexpression of Native Ferritin Gene *MusaFer1* Enhances Iron Content and Oxidative Stress Tolerance in Transgenic Banana Plants.” *PLoS One* 12: e0188933.

Ye, X., S. Al-Babili, A. Klöti, et al. 2000. “Engineering the Provitamin A (β-Carotene) Biosynthetic Pathway Into (Carotenoid-Free) Rice Endosperm.” *Science* 287: 303–305.

Zhang, Y., Y. H. Xu, H. Y. Yi, and J. M. Gong. 2012. “Vacuolar Membrane Transporters OsVIT1 and OsVIT2 Modulate Iron Translocation Between Flag Leaves and Seeds in Rice.” *Plant Journal* 72: 400–410.

Zhou, R., S. Wang, N. Zhan, et al. 2024. "High-Quality Genome Assemblies for Two *Australimusa* Bananas (*Musa* spp.) and Insights Into Regulatory Mechanisms of Superior Fiber Properties." *Plant Communications* 5: 100681.

Zhou, X., S. Li, Q. Zhao, et al. 2013. "Genome-Wide Identification, Classification and Expression Profiling of Nicotianamine Synthase (*NAS*) Gene Family in Maize." *BMC Genomics* 14: 238.

Supporting Information

Additional supporting information can be found online in the Supporting Information section.